

Tribochemical Interactions between a Polymer Composite and Metals

**Investigation of Tribochemical Interactions between a
PTFE Filled Composite and Common Industrial
Metals**

By Wing Hei Lam, B.Eng

A thesis submitted to the School of Graduate Studies in partial fulfilment of the
requirements for the degree of Master of Applied Science

McMaster University

©Copyright by Wing Hei Lam, April 2017

Lay Abstract

The field of friction, wear and lubrication, also known as tribology, traditionally focuses on metal and ceramic components that have high maintenance and lubrication costs. In recent years, there has been growing interest in plastic composites as a replacement material for tribological applications. The high strength, light weight, chemical resistance and self-lubricating properties of these plastic composites makes them an attractive substitute for metals and ceramics. Understanding the chemical interaction between plastic and metal during sliding is necessary to exploit their properties and performance for specific applications. In this study, a plastic composite based on a blend of polyphenylene ether (PPE) and high impact polystyrene (HIPS) filled with polytetrafluoroethylene (PTFE), carbon black and carbon fiber was used to investigate the effects of different metals on tribological performance and behaviour. Four common metals used in industry were chosen for this study: carbon steel C1018, naval brass 485, Inconel 625 and stainless steel 316. The tribology tests conclusively showed that friction and wear results differ between polymer-metals systems, with each system displaying a stable and unstable behaviour. Surface analysis revealed that the surface PTFE morphology of the polymer composite and the transfer film composition on the metal washer also differ between metals. Tribochemical reactions and the reactivity of each metal explained the results and behaviour of each polymer-metal system.

Abstract

The high specific strength, chemical resistance and processability of polymer composites have made them an attractive alternative to traditional metals and ceramics in many industries. For tribological applications, polymer composites also have the ability to eliminate the need of lubricants and lower maintenance costs. The use of carbon fiber, carbon black and polytetrafluoroethylene (PTFE) are well established in the literature as effective reinforcement agents and solid lubricants respectively but not many studies have explored the tribochemical interactions that occurs during sliding. This study investigates the tribochemical interactions between a polyphenylene ether (PPE) and high impact polystyrene (HIPS) blend based composite and different metal surfaces. Four common metals used in industry were chosen for this study: carbon steel C1018, naval brass 485, Inconel 625 and stainless steel 316.

In order to isolate the effect of tribochemical interactions between the polymer composite and counterface metals, consistent pressure and velocity (PV) settings were used for all tests. Frictional forces and temperature data were recorded during testing and the wear rates were determined by weighing samples before and after testing. The polymer sand metal washer surfaces were then examined under scanning electron microscopy (SEM) and energy dispersive spectroscopy (EDS) for their PTFE surface morphology and transfer film composition, respectively. The surface roughness of both polymer and metal samples were also measured.

It was observed that tribological performance of the polymer composite was affected by the composition of the metal counterface, and each metal had a different tendency to operating in a stable and unstable state. The surface morphology of the PTFE phase and the transfer film composition on the metal washers also differed between each polymer-metal system. SEM

micrographs reveal agglomeration of PTFE domains on the polymer surface and each system had a different domain size distribution and PTFE surface coverage.

The polymer-brass system was found to be the most consistent and give the most stable operations with the highest PTFE coverage on the polymer sample's surface due to brass' relatively high reactivity. This was explained by tribochemical reaction that occurs at the interface and the reactivity of each metal alloy. Adhesion must be high in order to enable a thicker and more uniform transfer film to adhere, which provides a smooth asperity-free surface for the polymer to slide against, resulting in a stable and low wear operation. A reactive interface allows the introduction of carboxyl groups on both the surfaces and increase electrostatic adhesion between the polymer transfer film and metal surface. Overall, the reactivity of each metal alloy correlated well with the number of stable tests that each polymer-metal system demonstrated as well as the resulting surface coverage of PTFE. This was taken as evidence of the tribochemical interactions.

Acknowledgements

I would like to thank Dr. Michael R. Thompson for his patience, mentorship and guidance during my studies. It was him who founded my interest in the field of polymer engineering and processing during my undergraduate studies and without him I wouldn't be where I am now. I also want to thank him for this tremendous opportunity to study and work with him on several interesting industrial projects. I've not only learned technical skills but also many soft skills during my studies under Dr. Thompson. I also appreciate the amount of time and effort he devotes to his students despite his busy calendar.

I would also like to thank everyone who's been through the last 2 years with me. I would like to express my appreciation for Dr. Emily Cranston, Dr. Li Xi and Elizabeth Takacs for their guidance during different points in my studies. I thank Dr. Maryam Emami who I worked with for most of the past 2 years for her input and perspective. A big thank you to Paul Gatt and Mike Clark for their patience and technical help, without their expertise my work would not have been possible. I also want to thank my friends and colleagues in and out of the department who've given me their time, advice and support.

I also like to thank NSERC, OCE and McMaster University for the financial support in this project. Thank you to the chemical engineering departmental staff who handles all the administrative work so I can focus on my work. To the staff at CCEM, in particular Glynis de Silveira and Chris Butcher, thank you for the training, advice and help with this project.

Finally I would like to thank my family and close friends for their constant love, encouragement and support through the bad times and the good. I would never have made it this far without all of you.

Table of Contents

Lay Abstract.....	ii
Abstract.....	iii
Acknowledgements.....	v
Table of Contents.....	vi
List of Figures.....	viii
List of Tables.....	xii
Abbreviations.....	xiii
Chapter 1 Introduction.....	1
1.1 Background.....	1
1.2 Research Objectives.....	3
Chapter 2 Literature Review.....	4
2.1 Introduction.....	4
2.2 Metal vs. Polymer Tribology.....	5
2.3 Wear Mechanisms.....	6
2.4 Role of Composites as Tribological Materials.....	7
2.5 Importance of Transfer Film.....	9
Chapter 3 Experimental.....	12
3.1 Materials.....	12
3.2 Sample Preparation.....	13
3.3 Tensile Test.....	15
3.4 Differential Scanning Calorimeter.....	15
3.5 Tribology Tests.....	15
3.6 Scanning Electron Microscopy.....	16

3.7 Surface Roughness	18
3.8 Hardness Testing	18
Chapter 4 Results	19
4.1 Physical properties of the composite material and metals	19
4.2 General Tribology Results	23
4.3 Carbon Steel C1018 Results.....	27
4.4 Brass Results	31
4.5 Inconel Results	34
4.6 Stainless Steel 316SS Results	39
Chapter 5 Discussion	43
5.1 Condition for stability	43
5.2 Carbon Steel C1018 System.....	46
5.3 Brass System	47
5.4 Stainless Steel 316SS System	48
5.5 Inconel System	49
Chapter 6 Conclusion.....	50
References.....	52
Appendix.....	55

List of Figures

Figure 1 - Tribochemical reaction between PTFE and metal surface adapted from Jintang (Jintang 2000).	10
Figure 2 - Schematic used for machining polymer samples, dimensions in mm.	14
Figure 3 - Schematic used for machining metal washers, dimensions in mm.	14
Figure 4 - Illustration of how the transfer film is split into quarters. Black lines show the division between each quarter.....	17
Figure 5 - DSC curve of the HIPS/PPE based composite. The marked temperature is the T_m of PTFE.	19
Figure 6 - Hardness of the investigated materials. *All metals were tested on the Rockwell B scale while the polymer sample was tested on the Shore D scale.	20
Figure 7 - Surface roughness values of unworn polymer sample and metals prior to testing.	21
Figure 8 – (a) SEM backscatter electron composition image of sanded but unworn polymer surface with PTFE domains highlighted in red. (b) The normalized size distribution from $50 \mu\text{m}^2$ to $1,000,000 \mu\text{m}^2$ of unworn polymer surface.	22
Figure 9 - Typical friction and temperature curves from tribology tests.	24
Figure 10 - Average results for each polymer-metal tribology system.	25
Figure 11 - Surface roughness values of unworn polymer sample compared to worn polymer samples for each polymer-metal system.	26
Figure 12 - Surface roughness of unworn metal washers compared to worn metal washers along and across the wear track.	26
Figure 13 - Typical CoF and temperature curve of stable and unstable C1018 tests.	28
Figure 14 - Average results of stable and unstable C1018 system tests.	28

Figure 15 - (a) SEM backscatter electron composition image of C1018 polymer sample surface under stable conditions with PTFE domains highlighted in red and (b) the associated normalized size distribution from 50 μm^2 to 1,000,000 μm^2 of C1018 polymer sample surface under stable conditions. (c) SEM backscatter electron composition image of C1018 polymer sample surface under unstable conditions with PTFE domains highlighted in red and (d) the associated normalized size distribution from 50 μm^2 to 1,000,000 μm^2 of C1018 polymer sample surface under unstable conditions..... 30

Figure 16 – Comparison of transfer film composition on C1018 washer between a stable and unstable sample. 1st quarter is the inner circumferential quarter while the 4th quarter is the outer circumferential quarter..... 30

Figure 17 - Typical CoF and temperature curve of stable and unstable brass tests..... 31

Figure 18 - Average results of stable and unstable brass system tests..... 32

Figure 19 - (a) SEM backscatter electron composition image of brass polymer sample surface under stable conditions with PTFE domains highlighted in red and (b) the associated normalized size distribution from 50 μm^2 to 1,000,000 μm^2 . (c) SEM backscatter electron composition image of brass polymer sample surface under unstable conditions with PTFE domains highlighted in red and (d) the associated normalized size distribution from 50 μm^2 to 1,000,000 μm^2 33

Figure 20 - Comparison of transfer film composition on brass washer between a stable and unstable sample. 33

Figure 21 - Typical CoF and temperature curve of stable and unstable Inconel tests..... 35

Figure 22 - Average results of stable and unstable Inconel system tests..... 35

Figure 23 - (a) SEM backscatter electron composition image of Inconel polymer sample surface under stable conditions with PTFE domains highlighted in red and (b) the associated normalized size distribution from 50 μm^2 to 1,000,000 μm^2 37

Figure 24 - (a) SEM backscatter electron composition image of Inconel polymer sample surface under unstable conditions at the peak CoF value with PTFE domains highlighted in red and (b) the associated normalized size distribution from 50 μm^2 to 1,000,000 μm^2 . (c) SEM backscatter electron composition image of Inconel polymer sample surface under unstable conditions at the valley CoF value with PTFE domains highlighted in red and (d) the associated normalized size distribution from 50 μm^2 to 1,000,000 μm^2 38

Figure 25- Comparison of transfer film composition on Inconel washer between a stable and unstable sample at the peak and valley positions of the CoF curve..... 39

Figure 26 - Typical CoF and temperature curve of stable and unstable 316SS tests..... 40

Figure 27 - Average results of stable and unstable 316SS system tests. 40

Figure 28 - a) SEM backscatter electron composition image of 316SS polymer sample surface under stable conditions with PTFE domains highlighted in red and (b) the associated normalized size distribution from 50 μm^2 to 1,000,000 μm^2 . (c) SEM backscatter electron composition image of 316SS polymer sample surface under unstable conditions with PTFE domains highlighted in red and (d) the associated normalized size distribution from 50 μm^2 to 1,000,000 μm^2 41

Figure 29 - Comparison of transfer film composition on 316SS washer between a stable and unstable sample..... 42

Figure 30 - Fiber reorientation under friction and wear with arrow indicating direction of sliding.
..... 44

Figure 31 - Proposed tribochemical reaction mechanism between polymer and metal adapted from Jintang and Onodera et al (Jintang 2000; Onodera et al. 2014). PTFE was used as an example for its ease of transfer and simplicity.....	46
Figure 32 - CoF and temperature curve of an unstable C1018 test.	47
Figure A1 - Tribometer fabriacted specifically for this study.....	55
Figure A2 - Close up view of a mounted sample.....	56
Figure A3 - Unworn polymer sample and C1018 Washer	56
Figure A4 - Worn polymer sample and C1018 washer.	57
Figure A5 - LabView program main screen.	57

List of Tables

Table 1 - Composition, hardness, thermal conductivity and density values of metals (Materials 2012; McMasterCarr 2016a; McMasterCarr 2016c; McMasterCarr 2016b).	13
Table 2 - Mechanical properties of HIPS/PPE based composite material.....	19
Table A1 - Comparison of average CoF and absolute wear of polymer-metal system	58

Abbreviations

PPE	Polyphenylene Ether
HIPS	High Impact Polystyrene
PTFE	Polytetrafluoroethylene
CoF	Coefficient of Friction
PV	Pressure-Velocity
SEM	Scanning Electron Microscopy
EDS	Energy Dispersive Spectroscopy
PEEK	Polyether Ether Ketone
DSC	Differential Scanning Calorimeter
BEC	Backscatter Electron Composition
Ra	Roughness Average
MD	Molecular Dynamics
QCMD	Quantum Chemical Molecular Dynamics
MO	Metal Oxide
MF	Metal Fluoride
HF	Hydrogen Fluoride

Chapter 1 Introduction

1.1 Background

Polymeric materials are gradually replacing their traditional metal and ceramic counterparts that have been well studied in tribological applications (Petrica et al. 2015; Brostow et al. 2010). In order to improve the usability of polymers in a wider range of applications, more knowledge and research on their performance and behaviour is required (Brostow et al. 2010). From the aspect of the user, engineering plastics can lower operational costs, maintenance demands, part weight, and eliminate the need of lubricants compared to traditional metal and ceramic materials (Brostow et al. 2010). Compared to traditional commodity plastics, engineering plastics are stronger, more chemically resistant and have higher specific strength on account of their light weight than those traditional materials (Lee et al. 2007). Moreover, engineering polymers have higher formability than metals and ceramics making them an attractive material for manufacturers (Konovalova et al. 2012). Intricate and complex shapes can be made easier and faster using injection molding and extrusion as opposed to standard machining and stamping methods for metals and ceramics (Konovalova et al. 2012). These advantages are universal across many industries and are desired by engineers if a product is available for their application and requirements.

Polymer composites are needed for harsh environments and applications where unfilled polymers would not fulfill the tribological, mechanical and temperature requirements. Reinforcement agents and solid lubricants, such as carbon fiber and Polytetrafluoroethylene (PTFE), are popularly used in composites to improve wear resistance and coefficient of friction for high pressure and velocity (PV) limits (Conte & Igartua 2012). Carbon fibers not only improve

mechanical properties but also act as the load bearing element against the counterface and rolling asperities and thereby improve wear resistance (Zhao, Hussainova, Antonov, Wang, & Wang, 2012.). If good interfacial adhesion is achieved between a polymer matrix and such fillers then stresses can be transferred more effectively to further enhance stiffness, surface hardness and wear resistance (Zhou et al. 2013).

Solid lubricants like PTFE are able to lubricate a moving interface and form a transfer film to further lower friction by enabling the sliding between polymer chains compared to a polymer-metal interface which has higher friction (Jintang 2000; Chiu et al. 2012). This feature, unique to viscoelastic polymeric materials, allows the elimination of lubricants while maintaining high tribological performance (Konovalova et al. 2012). The interaction between polymer and metal counterface are often recognized but not investigated as the tribochemical effects are complex and different for each material system and its' operating conditions (Jintang 2000). Bahadur suggests that there is a combination of coulomb electrostatic forces, Van der Waals forces and chemical bonding between the transfer film and metal surface (Bahadur 2000). Jintang suggested creation of metal fluorides and bonding of polymer chain to the metal surface when enough mechanical and thermal energy is present (Jintang 2000). Although the mechanisms and reaction behind it are complex, Bahadur reported a strong correlation between transfer film bond strength and wear resistance of the system (Jintang 2000; Bahadur & Sunkara 2005). Since the bond strength is dependent the polymer transfer film and the mating surface, there is a need to understand the interaction between a polymer and different metal counterfaces.

Currently, tribological performance of polymer composites have been researched under various sliding velocity and pressures but with no comparative studies of numerous metals as the contacting counterface. Without examining the tribochemical effects taking place at the contacting

faces of polymer-metal systems, polymer composites cannot be truly optimized for the various applications in which they are currently deployed. The tribological performance can be greatly affected by tribochemical effects and thereby limiting the adoption of polymer composite as tribological materials. The following thesis explores the effect of different metal counterfaces on tribological performance of a PPE+PS blend based composite under the same PV conditions.

1.2 Research Objectives

1. To explore the physiochemical effects of counterface materials on the tribological behaviour and performance of a composite material
2. Explain the different interactions between transfer film and multiple metal counter surface
3. Relate transfer film characteristics to friction and wear behaviour

Chapter 2 Literature Review

2.1 Introduction

Tribology is the study of friction, wear and lubrication of interacting surfaces that are in relative motion (Williams 2005). It is derived from the Greek word “Tribos” which mean rubbing. Friction is caused by the resistance to relative motion of two contacting interfaces (Findik 2014). Wear is the material lost due to damage by the opposing relative motion between two contacting surfaces (Williams 2005). Polymers and their composites are gradually replacing metals and ceramics in tribological applications and to improve them, their frictional and wear behaviour must be further researched (Brostow et al. 2010; Petrica et al. 2015).

Many different testing configurations exist but when testing polymers, the most used configuration in the literature is “pin on disk”, with the polymer as the pin and the metal as a rotating disk (Unal et al. 2004; Novak & Polcar 2014; Zhang et al. 2015a; Tzanakis et al. 2013; Tanaka et al. 1973). Pressure (P) and sliding velocity (V) are the main variables of study with the duration described in units of time or sliding distance. The pressure is usually supplied using a dead weight to ensure that the same normal force is applied throughout the test. The product of pressure and sliding speed is the Pressure-Velocity (PV) factor that describes friction and wear tests. Pressure is an important factor for polymers as they can deform and eventually fail under loads that metals can cope with. Therefore, besides the coefficient of friction and wear resistance, polymers can be evaluated based on their PV limit.

The *coefficient of friction* (COF) is calculated by simply dividing the tangential (frictional) force by the normal force. Both forces can be obtained using a multi-axis load cell that measure friction force and normal force in the x, y, and z directions (Sawyer et al. 2003). *Wear* is the

measured difference in mass of the sample, before and after testing, and can be reported either as mass or volume loss over time or over sliding distance. Alternatively, a *specific wear rate*, k , can be calculated using the following equation where V_L is the volume lost, F_n is the normal force and D is the sliding distance (Lancaster 1969):

$$k = \frac{V_L}{F_n D} \quad (1)$$

2.2 Metal vs. Polymer Tribology

The frictional behaviour of metals and polymers are vastly different. Metals rely on lubricants to operate while some polymers are able to self-lubricate via a transfer film mechanism, eliminating the need of a lubrication system. Although wear mechanisms are very similar, the dominant mode of wear is different between polymers and metals. Metals are more susceptible to corrosive wear whereas polymers experience more adhesive wear. That is not to say adhesive wear is uncommon between metals. In fact, when similar metals are in contact, the weaker material will always transfer to the stronger one but often surface oxide layers and lubricants prevent this by providing a boundary layer between the two that will substantially reduce or even eliminate adhesive wear (Findik 2014). Moreover, metals can experience oxidation, seizure and melt wear mechanism that aren't common in polymers (Williams 2005). Due to the soft and elastic nature of polymers, they are more impact resistant compared to popular soft metals like brass and aluminum. This also affects the real contact area causing some polymers to not follow common laws of friction like metals, as the polymer surface can deform under pressure. The resulting increased contact area can increase the coefficient of friction, which violates Amonton's second law of friction. Zhang et al. reported differences in friction coefficients between polyether ether ketone (PEEK) based composite materials and 100Cr6 steel discs when conducting their experiment at different pressures (Zhang et al. 2015b). Another limitation is Amonton's third law, also known as

Coulomb's law of friction, which does not account for the adhesion between surfaces which polymers can exhibit while sliding with high interfacial temperatures. Buckley stated that many experimental investigations exhibit an elevated amount of adhesion between polymer and metal (Buckley 1981). Temperature effects are also more dominant in polymer tribology due to the relatively low thermal conductivities and softening temperatures of the materials. Thermal energy generated during sliding can decrease the wear resistance, load carrying capacity and increase adhesive wear limiting polymeric materials to low temperature applications. At the same time, the thermal energy and shear causing physical damage to the polymer is also able to change crystallinity and the orientation of polymers chains (Conte et al. 2013; Liu et al. 2005).

2.3 Wear Mechanisms

There are four main wear mechanisms in polymer tribology: abrasive cutting, fatigue, adhesion and tearing (Brostow et al. 2010; Williams 2005). Abrasive cutting and fatigue are usually the dominant factors in the wear of semi-crystalline and amorphous polymer systems. Abrasive cutting occurs when asperities on the harder material is able to cut into the softer material and a ploughing effect occurs, causing wear and damage to the surface. This is known as two-body abrasion (Myshkin et al. 2005). This cutting effect is usually the dominant wear mechanism in the short term as there isn't enough thermal energy yet for the other mechanisms (Eiss & Potter 1985). In a polymer-metal tribology system the metal is usually the harder material and any surface features will increase initial wear of the polymer until the metal is polished by the polymer or its fillers. Three-body abrasive cutting occurs when wear particles in the interface causes abrasive wear to either or both surfaces (Myshkin et al. 2005). This is commonly caused by detached polymer fillers or metal particles that are unable to escape the interface.

Fatigue is a thermally activated process that causes oxidative and thermal degradation of the polymer's wear surface (and sub-surface) and is usually the dominant wear mechanism in steady-state wear (Eiss & Potter 1985). Chemical bonds and chains are broken and cracks initiate and propagate through the surface and sub-surface. It is known that cracks initiate and propagate where the highest concentration of stress is located (Myshkin et al. 2005). This can be scratches, voids or poor polymer-filler interfaces where load transfer occurs in polymer composites (Myshkin et al. 2005; Tzanakis et al. 2013). As bonds and chains are broken, heat is released and thus increases local temperature at the interface, which promotes adhesive wear. Chains with more energy and mobility are able to detach from the bulk and attach, mechanically and chemically, to the counterface. For this to happen the bonding energy between surfaces must be higher than the local bonding energy of the chains. Once this criteria is satisfied adhesive wear occurs (Myshkin et al. 2005). Tearing is caused by initiation and propagation of sub-surface cracks due to fatigue from cyclic loading (da Silva et al. 2007). The thermal energy released from abrasive wear at the surface accelerates the growth of sub-surface cracks until they propagate to the surface and shear forces tear away large sheets of material (da Silva et al. 2007).

2.4 Role of Composites as Tribological Materials

Reinforcing fillers are traditionally used to increase mechanical properties of polymer composites. In tribology systems they can decrease friction and wear if good interfacial adhesion is present with their polymer matrix. In the case of poor interfacial adhesion, wear will increase as fillers are more easily detached from the polymer matrix and increasingly produce three-body abrasive wear. They decrease friction and wear by creating small bumps on the surface causing the real contact area to be smaller than the apparent area. Fillers like carbon fiber and carbon black can also become the load bearing element in the composite as they are stronger and more wear

resistant than the polymer matrix (Zhao et al. 2012). Currently, carbon fibers with a diameter of 7 μm and length between 50 μm and 230 μm are commonly used in polymer composites for studying its effect on friction and wear performance as they are popularly used in industry (Yamamoto & Hashimoto 2004; Zhao et al. 2012; Zhang 2011; Wenzhong 2015a). They improve surface hardness and stiffness of the polymer by improving load transfer between fiber and polymer matrix (Zhou et al. 2013). With improved load transfer and material strength, the load bearing capacity is increased, thus enabling the material to achieve higher PV limits (Lancaster 1972).

Due to the inherent strength of fibers and other reinforcing fillers, they can also cause abrasive wear to the counterface. Depending on the counterface surface hardness, this can increase surface roughness and thus increasing frictional heat generation. This in turn can cause temperatures to rise above the polymer's glass transition temperature (Tzanakis et al. 2013). When that occurs, the interfacial adhesion between matrix and filler is weakened and thermal degradation is promoted (Tzanakis et al. 2013). Weakly attached fillers can then detach from the polymer and cause either increased three body abrasive wear, as previously mentioned, or decrease actual contact area by acting as a rolling element to decrease friction or both, depending on the contact pressure and material properties (Tzanakis et al. 2013).

Solid lubricant fillers, such as PTFE, can be added to decrease friction. Their surface energy is low which causes adhesion at the interface to be low and thus decreasing friction. Polymeric lubricants, like PTFE, can form a transfer film on the counterface to lower friction. These materials often make the polymer more susceptible to abrasive wear if large amounts are added. Moreover, due to the soft nature of materials like PTFE, wear particles can easily penetrate the surface and turn it into an abrasive surface for wearing away the counterface (Myshkin et al. 2005). Being a polymer also makes PTFE more susceptible to thermal degradation and fatigue

compared to inorganic fillers. Tzanakis et al. reported a decrease in toughness and increase in crack growth within the PTFE phase of a polymer matrix due to thermal degradation from the heat generated during their tests (Tzanakis et al. 2013). Crystallinity changes in the PTFE phase can also affect its performance as a solid lubricant (Conte et al. 2013; Liu et al. 2007). Liu et al. reported that reorientation of PTFE chains can occur when enough thermal energy is present for the chains to be mobile and friction is lowest and most stable when orientation direction matches that of sliding direction (Liu et al. 2007).

2.5 Importance of Transfer Film

It is well known that the transfer film in a polymer-metal tribology system is a key factor affecting its friction and wear behaviour and is what makes polymers self-lubricating (Bahadur 2000; Jintang 2000). The conditions for transfer to occur is the same as adhesive wear, where the interfacial associations between polymer and metal are stronger than bonding between chains in the bulk polymer material, but the adhered material is not abrasively worn away after being attached (Myshkin et al. 2005). Mechanical interlocking can occur to further strengthen the adhesive strength of the transfer film (Bahadur 2000). The existence of the transfer film shields the soft polymer from the hard asperities of the metal surface and enables easy sliding between polymer chains to lower wear and friction respectively (Jintang 2000; Bahadur 2000). Bahadur found that nylon had 4 times better wear resistance if a high quality transfer film was formed highlighting the pronounced effect transfer film has on wear behaviour (Bahadur 2000). PTFE have been reported to form transfer films easily making it a very popular low friction additive in polymer composites (Bahadur 2000). Tanaka et al. reported that the banded crystal structure of PTFE can be easily destroyed, due to its low activation energy of 29kJ/mol, and slippage of crystalline slices can occur (Tanaka et al. 1973). Jintang suggested that at the same time C-C or C-

F covalent bonds are broken and fluorine ions can react with metal oxides or the metal surface to chemically bond, as seen in Figure 1 below (Jintang 2000). Since radicals are present back-transfer can occur by adhering or polymerizing with the bulk polymer or its fillers (Myshkin et al. 2005).

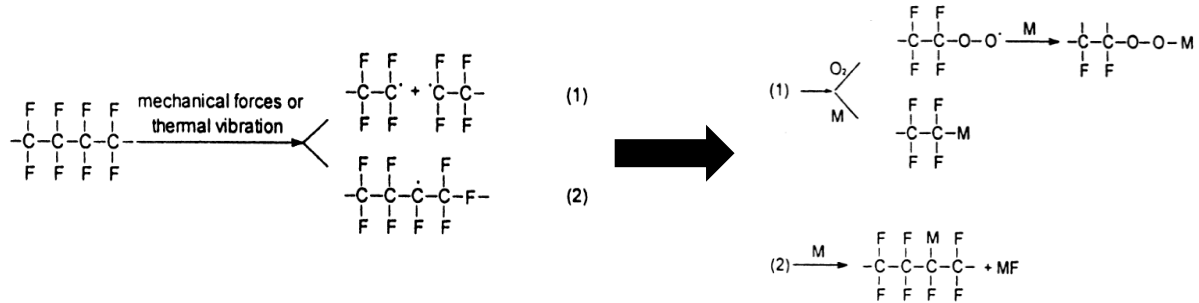


Figure 1 - Tribochemical reaction between PTFE and metal surface adapted from Jintang (Jintang 2000).

Transfer film thickness is dependent on the temperature, sliding speed and tribochemical interaction between polymer and metal (Bahadur 2000; Bahadur & Sunkara 2005; Myshkin et al. 2005). At moderate temperatures and sliding speeds the transfer film thickness is reported to be as thin as 10 nm but at higher temperature and sliding speed, the thickness can exceed 0.1 μm (Bahadur 2000). The counterface material plays a dominant role of whether a thick film is able to adhere and remain adhered amid adhesion and abrasive wear (Myshkin et al. 2005). Bahadur explained that if the adhesion between transfer film and counterface is weak, the film can be peeled off becoming wear debris stuck in the interface and possibly causing three body abrasion (Bahadur 2000). Halley and Mackay reported brass surfaces have pits that allow polymers to entangle and adhere to its surface resulting in more stable flow behaviour during extrusion experiments compared to stainless steel (Halley & Mackay 1994). This is applicable as the polymer surface at the interface can be at temperatures above its glass transition temperature giving chains the

mobility and energy to behave in a melt like state. Myshikin reported that the transfer film formed between PTFE and steel substrate would have an oscillating thickness showing that the top layers of transfer film can be removed and replaced during sliding (Myshkin et al. 2005).

Chapter 3 Experimental

3.1 Materials

A polymer composite was used as the reference material for the study. The matrix polymer was a 12 MVR (280 °C/5 kg; ISO 1133) amorphous engineering polymer consisting of a miscible blend of high impact polystyrene (HIPS) and polyphenylene ether (PPE) in the form of pellets was used. The neat HIPS/PPE was filled with polytetrafluoroethylene (PTFE), carbon fibers and carbon black powder at weight proportions of 17.5%, 10% and 5%, respectively. The supplied PTFE powder had a nominal feret particle diameter of 9 μm ; the carbon fibers exhibited a nominal diameter and length of 7.4 μm and 150 μm ; the lamp black carbon black powder had a nominal feret particle diameter of 10 μm . The aforementioned carbon fiber was chosen as they fall within the popular dimension range, diameter of 7 μm and length between 50 μm and 230 μm , used in polymer composite tribological studies (Yamamoto & Hashimoto 2004; Zhao et al. 2012; Zhang 2011; Wenzhong 2015b). The resultant composite has a density of $1.227\pm 0.04 \text{ g/cm}^3$. The HIPS/PPE based composite was chosen because amorphous polymer based composites are not popularly investigated in literature and the fact that mechanical strength does not rely on crystal orientation makes it attractive for applications where in-plane isotropic strength is required. The additives were chosen to improve the tribological and mechanical properties of HIPS/PPE.

Four distinctly different metals were investigate to examine their effect on the performance of a polymer-metal tribologic system. Carbon steel 1018, stainless steel 316, naval brass 485 and Inconel 625 were used as the metal counterface in the form of washers. Table 1 below contains their composition, hardness, thermal conductivity and density data.

Table 1 - Composition, hardness, thermal conductivity and density values of metals (Materials 2012; McMasterCarr 2016a; McMasterCarr 2016c; McMasterCarr 2016b).

Carbon Steel C1018		485 Naval Brass		625 Inconel		Stainless Steel 316	
Material Composition		Material Composition		Material Composition		Material Composition	
Iron	98.81-99.26%	Copper	60%	Nickel	54.29-68.85%	Iron	58.23-73.61%
Maganese	0.6-0.9%	Zinc	36.7-38.1%	Chromium	20.00-23.00%	Chromium	16-18.5%
Carbon	0.15-0.2%	Lead	1.3-2.2%	Molybdenum	8.00-10.00%	Nickel	10-15%
Sulfur	0.05% Max	Tin	0.05-1.0%	Iron	5.00% Max.	Molybdenum	0-3%
Phosphorous	0.04% Max	Iron	0.10%	Niobium & Tantalum	3.15-4.65%	Manganese	0-2%
				Cobalt	1.00% Max.	Copper	0-1%
				Manganese	0.50% Max.	Silicon	0-1%
				Silicon	0.50% Max.	Titanium	0.7% Max.
				Aluminum	0.40% Max.	Nitrogen	0-0.1%
				Titanium	0.40% Max.	Carbon	0-0.08%
				Carbon	0.10% Max.	Sulfur	0.00%
				Other	0.165% Max.	Phosphorus	0-0.045%
Hardness	Rockwell B71		Rockwell B60		Rockwell B97		Rockwell B74
Thermal Conductivity (W/mK)	51.9		9.66		9.8		14.56-16.29
Density (g/cm ³)	7.87		8.45		8.59		8.04

3.2 Sample Preparation

The polymer composite was batch mixed using a Haake Rheomix 3000p for 10 minutes at 295 °C then grinded using a Rapid 66SRE granulator. Plates (9 cm x 9 cm x 6 cm) were made via compression molding by first pre-melting at 295 °C for 20 minutes before compressing to 3 MPa for 3 minutes. Samples were then machined out of the plates according to Figure 2 below.

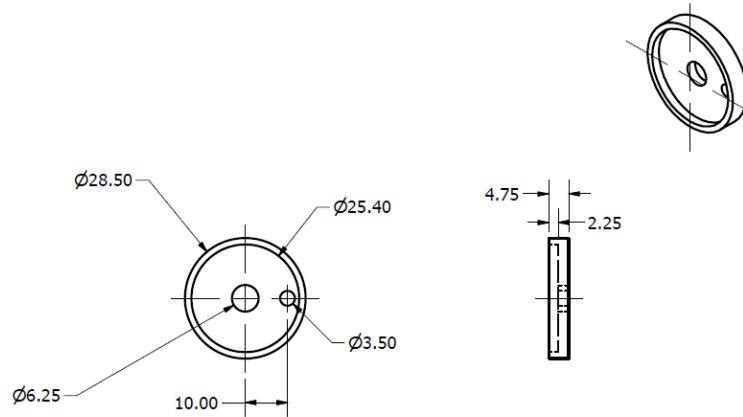


Figure 2 - Schematic used for machining polymer samples, dimensions in mm.

Tensile samples were compression molded to type IV dog bone samples as described in ASTM 638-14. Granules were pre-melted for 10 minutes at 295 °C before compressing to 3 MPa for 1 minute. The samples were then air cooled to room temperature.

Metal washers were machined out of billets with the dimensions described in Figure 3 below. A port was tap drilled on one side to a depth of 2.5mm to allow a thermocouple to be attached for monitoring the temperature of the system.

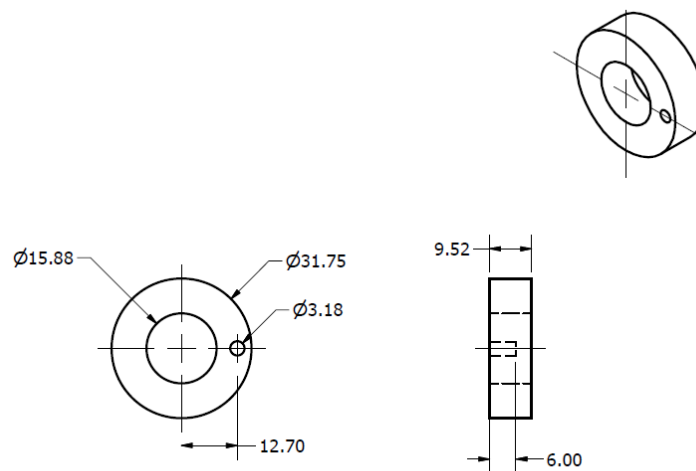


Figure 3 - Schematic used for machining metal washers, dimensions in mm.

3.3 Tensile Test

The tensile properties of the HIPS/PPE composite were determined using an Instron 3366 benchtop universal testing machine system (UTMS) in room temperature. The Type IV dog bones were tested using the procedure described in ASTM638-14 using a crosshead speed of 5mm/min. Five samples were used for each quoted measurement.

3.4 Differential Scanning Calorimeter

The thermal properties of the HIPS/PPE composite were determined using a Q200 differential scanning calorimeter (DSC) from TA Instruments. The Heat/Cool/Heat method was used for a temperature range of 20 °C to 380 °C with a heating rate of 10 °C/min and cooling rate of 10 °C/min under nitrogen purge.

3.5 Tribology Tests

Samples were tested with a vertical thrust type tribometer under 1.5 MPa of normal pressure. Before each test both polymer and metal samples are resurfaced with 600 grit sandpaper (Norton Blackice) using an infinity pattern 20 times to avoid sanding in a single direction. Each sample was run for 200±15 minutes at 80 rpm. Load was supplied by weights and monitored with a 50 Kg_f load cell (Omega LCM703-50). Friction was measured using a swing arm against a 10 Kg_f load cell (Omega LCM703-10). Frictional force was calculated with the following formula:

$$F = \frac{f \times d}{r} \quad (2)$$

The force (f) is measured at a distance d away from the center of rotation and must be scaled up using the radius between the inner and outer edge of the sample (r) to determine the actual frictional force (F) at the center of the contact patch. Coefficient of friction can then be calculated using Amonton's 1st law of friction below:

$$CoF = \frac{F}{W} \quad (3)$$

Where W is the normal force exerted on the sample. Temperature was monitored with a Type K thermocouple affixed to the metal washer. Sample and washer wear rates were determined by weighing them before and after each test. Tests were classified as stable if the CoF curve stabilizes around some value for a minimum of 60 minutes before the end of the test.

3.6 Scanning Electron Microscopy

Sample surfaces were examined using a JEOL 6610LV scanning electron microscope (SEM) equipped with energy dispersive spectroscopy (EDS) capabilities. Two different settings were used for imaging polymer samples and metal washers due to their large differences in conductivity. Polymer samples were imaged in a low vacuum environment of 30Pa with a 12kV electron beam while metal washers were imaged in a high vacuum environment with a 5kV electron beam. EDS data was captured and quantified using INCA software (Oxford Instruments).

Transfer film composition was approximated by EDS using the following formula which ignores the weight contribution from oxygen and hydrogen in the HIPS/PPE resin. This assumption had to be made as the proportion of HIPS to PPE used in the commercial resin was not known. Carbon contributions from the metals were negligible as their carbon content was very low, as reported in Table 1. Carbon signals from carbon fiber and carbon black is also ignored as neither was observed in SEM images.

$$wt\% PTFE = \frac{Fl}{C} \div \frac{2(18.998)}{12.011} \quad (4)$$

Fl and C are the weight percent of fluorine and carbon obtained from EDS data and the second fraction of the equation is the molar mass ratio of fluorine atoms to carbon atoms in PTFE.

Results are then averaged circumferential for each quarter width of the transfer film where the 1st quarter is the inner circumference and 4th quarter is the outer circumference, this is illustrated in Figure 4 below. Since EDS is a bulk measurement, the assumption of uniform composition is made during analysis. Due to the assumptions and the varying electron penetration depth, this is only to approximate and compare between samples and cannot be used as an absolute quantitative testing method for transfer film composition.

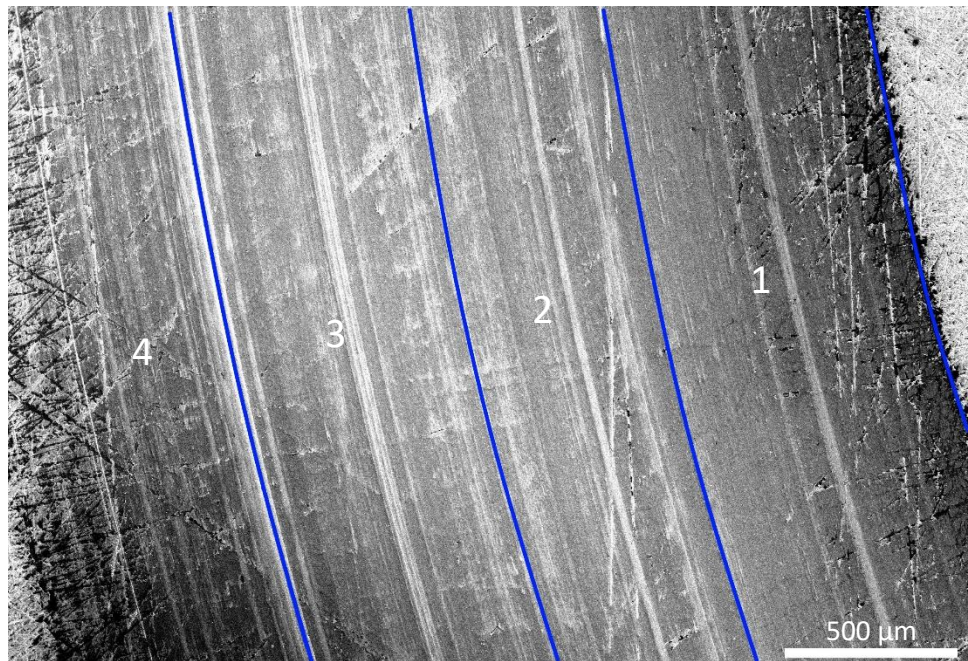


Figure 4 - Illustration of how the transfer film is split into quarters. Black lines show the division between each quarter.

The surface PTFE domain size analysis is conducted by processing backscatter electron composition (BEC) images using Gwyddion software. Since PTFE domain appears as white areas in the image, they were marked by using the Threshold function and a distribution is exported. Only domains larger than 3 μm^2 are included in generating the distribution to avoid false readings of metal debris embedded into the polymer surface. The surface coverage is calculated as the summation of the surface areas divided by the total area depicted by the image. The distributions

however are only shown from $50\mu\text{m}^2$ to $1,000,000\ \mu\text{m}^2$ as that is where the most significant changes are.

3.7 Surface Roughness

The surface roughness of samples and washers, before and after testing, was measured using a Mitutoyo SJ-210 surface roughness tester using the 0.03mm x 3 setting and a Roughness Average (Ra) value is reported. Five different spots was measured prior to testing for each metal and polymer sample along their contacting faces. For measurements after the test, eight different locations across the wear tracked was measured in both across and along the wear track for the washer and just along the contact patch for the polymer sample. The eight measurements were averaged and a nominal value was reported.

3.8 Hardness Testing

A Shored D hardness tester was used for polymer samples while a Rockwell hardness tester was used for the metal washers. Hardness testing of polymer samples was done according to the procedure described in ASTM D2240-05. Hardness testing of metal washers was done according to the procedure describe in ASTM E18-16.

Chapter 4 Results

4.1 Physical properties of the composite material and metals

Tensile testing was performed for the HIPS/PPE based composite at room temperature to define its mechanical properties. Table 2 below reports the results with uncertainty representing one standard deviation.

Table 2 - Mechanical properties of HIPS/PPE based composite material.

Modulus (MPa)	Toughness (MPa)	Max Strength (MPa)	Break Strain (%)
1277±82	0.895±0.121	37.3±1.9	4.44±0.38

DSC analysis was performed for the polymer composite. As the blend of HIPS and PPE is amorphous, there is no visible crystal melting transition until the crystals of PTFE started to melt at 330 °C. The T_g of the miscible blend is not visible but the Vicat softening temperature of the base resin is approximately 140 °C.

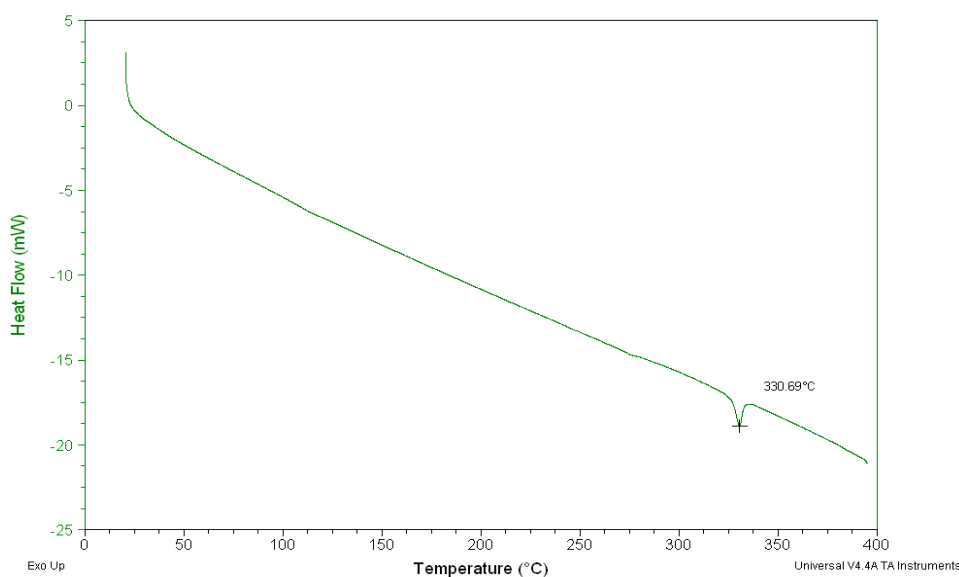


Figure 5 - DSC curve of the HIPS/PPE based composite. The marked temperature is the T_m of PTFE.

Hardness was tested for the composite and metals of interest. Figure 6 below reports the hardness values of each material, though on different scales. The polymer composite molded as a test specimen for friction was tested with a hardness tester and resulted in an average Shore hardness value of $D80.0 \pm 0.9$. All metal counterfaces prior to friction testing were evaluated for hardness and found to have higher surface hardness than specified in their datasheets. Carbon steel C1018 had an average Rockwell value of $B98.0 \pm 1.0$ compared to B71 from the specifications. Likewise Brass and stainless steel 316SS were tested to have an average value of $B78.0 \pm 1.4$ and $B91.0 \pm 0.8$ compared to the specified B60 and B74 hardness values, respectively. Inconel had the closest hardness value in comparison, with a tested average value of $B104.0 \pm 1.2$ which is comparable to the specified B97.

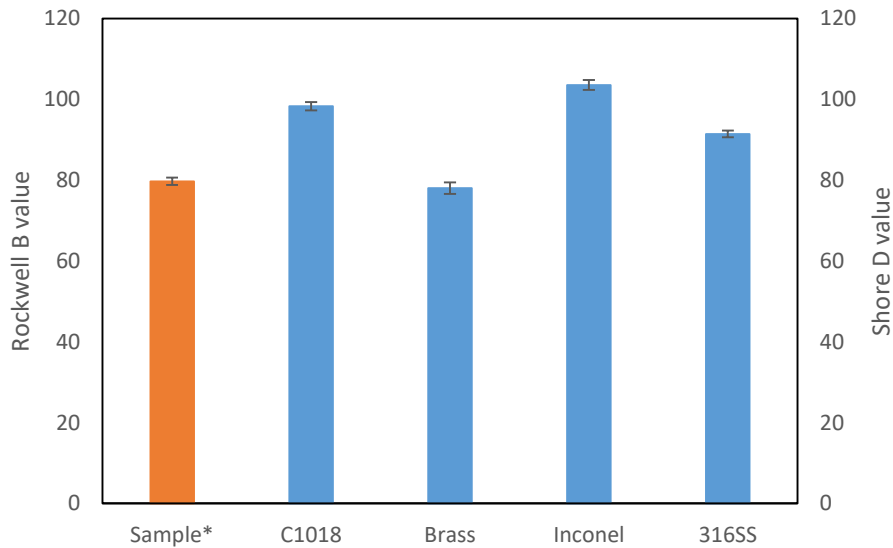


Figure 6 - Hardness of the investigated materials. *All metals were tested on the Rockwell B scale while the polymer sample was tested on the Shore D scale.

Samples were analyzed for their initial surface roughness. Figure 7 below shows that the surface roughness values of the polymer sample and metal washers decrease as the hardness, presented in Figure 2 above, increases thus finding an inverse relationship between surface

roughness and hardness for these materials. The polymer sample exhibited a high R_a value with a large error bar due to the relatively deep grooves resulting from sanding in preparation for friction testing. Metal surfaces were much smoother and more consistent in comparison due to their hard nature, despite also being prepared in the same manner.

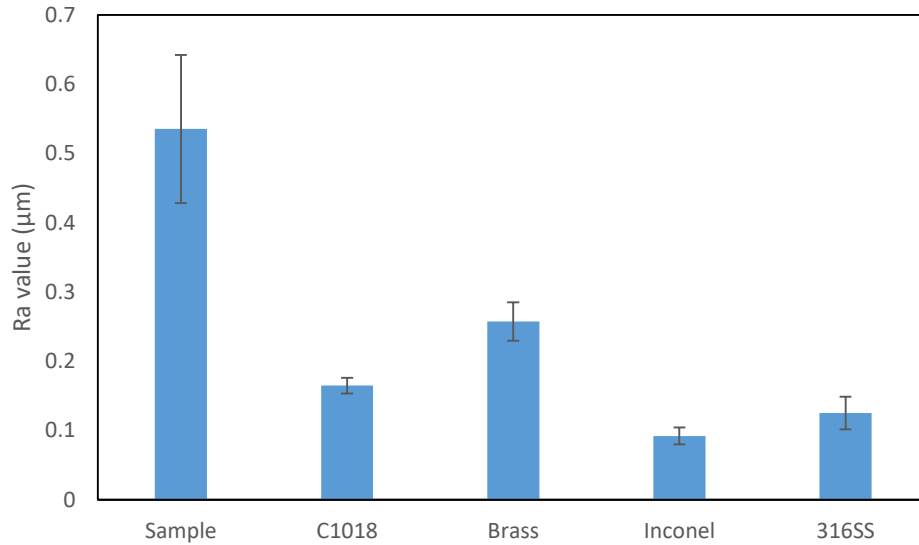


Figure 7 - Surface roughness values of unworn polymer sample and metals prior to testing.

Since the role of PTFE in lowering friction of a composite is of interest to this study, its surface domain size was examined. Figure 8 below shows the typical domain size and distribution of a sanded but unworn sample. The largest PTFE domains are below $1,000 \mu\text{m}^2$ and are well dispersed covering $9.13\% \pm 1.39\%$ of the surface. The normalized frequency of domain sizes ranging from $50 \mu\text{m}^2$ to $1,000,000 \mu\text{m}^2$ (1 mm^2) for the original composite is presented in Figure 4(b), with the x-axis scale setup for comparison with worn samples to be presented later in the discussion.

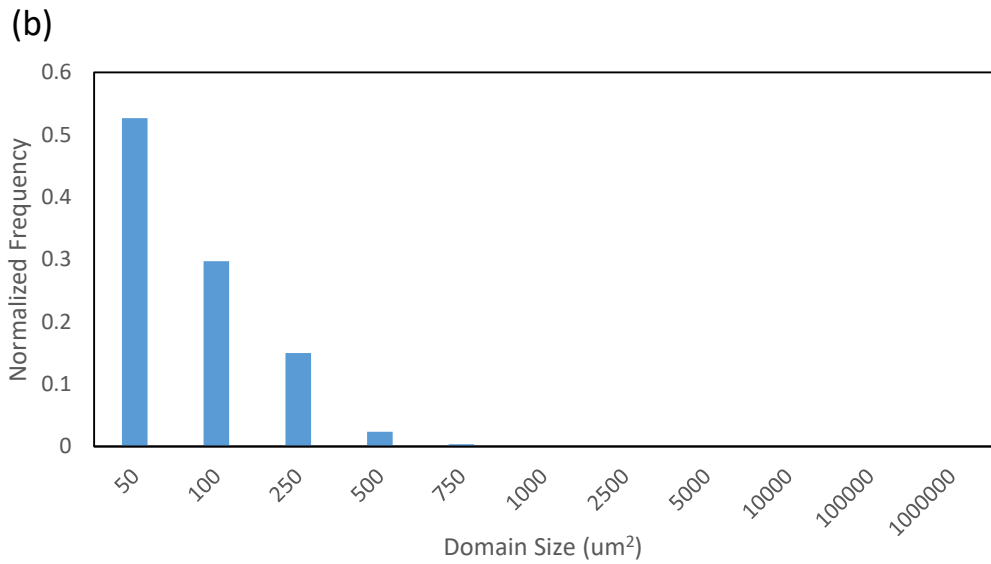
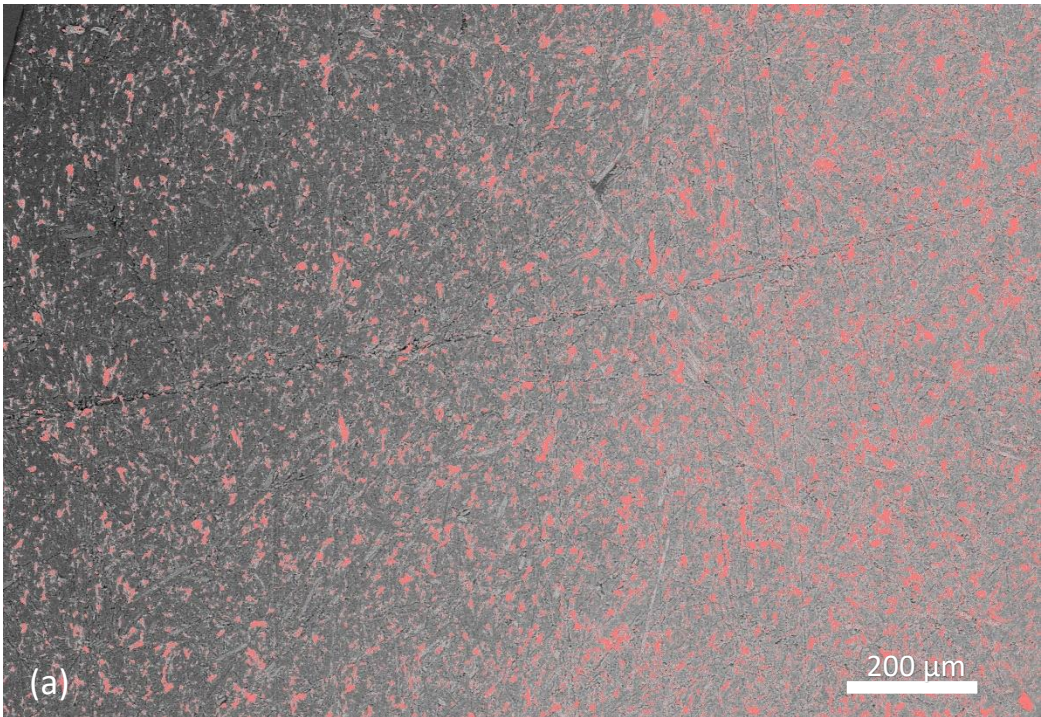


Figure 8 – (a) SEM backscatter electron composition image of sanded but unworn polymer surface with PTFE domains highlighted in red. (b) The normalized size distribution from $50 \mu\text{m}^2$ to $1,000,000 \mu\text{m}^2$ of unworn polymer surface.

4.2 General Tribology Results

The tribology results of this work involving brass, Inconel and 316SS will be compared to the base case of C1018 carbon steel, in all instances, as it is the most commonly used steel type in reported studies with polymers. Figure 9 demonstrates the typical coefficient of friction (CoF) results obtained from tribology testing of the composite with each metal system. With the exception of 316SS all other friction curves quickly stabilized at a certain value. The Inconel system produced the lowest CoF followed by C1018 carbon steel and brass. Generally, higher friction generated more heat but the measured temperature did not correlate with the friction results due to the differences in the metals' thermal conductivity and dissipation properties. Brass tribology tests exhibited the lowest temperature, followed by C1018, Inconel and 316SS. The demonstrated 316SS CoF curve shows relatively large fluctuations with a short-term decline in CoF after an initial increase before rising again to a stable value. The magnitude and duration of the short-term decline (or dip) does vary from test to test but was always witnessed in all repeated tests. All metals exhibited some unstable behaviour which will be discussed in the following sections.

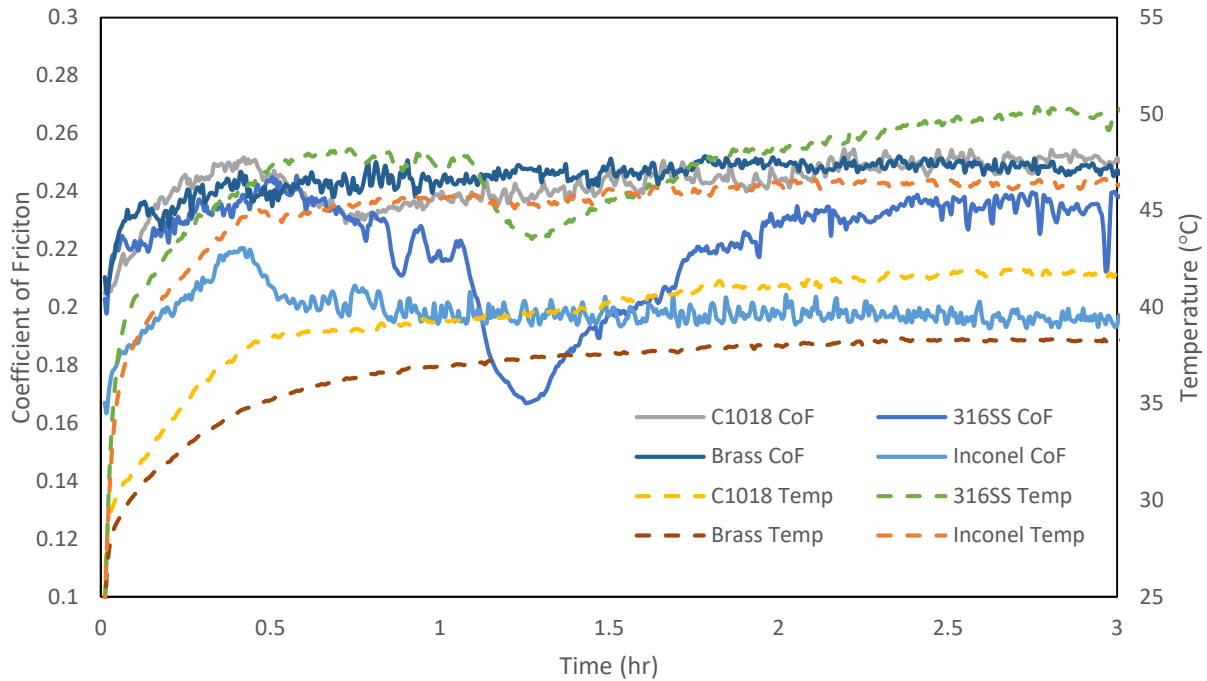


Figure 9 - Typical friction and temperature curves from tribology tests.

The average CoF, sample wear and washer wear of all conducted tests for each polymer-metal system are presented in Figure 10 - Average results for each polymer-metal tribology system. Wear is presented as a rate value assuming uniform losses from start to finish of a test. An average CoF per test was determined by averaging the calculated CoF throughout a test, while the average present in the figure is the average of average CoF found from all repeated trials. The average CoF results for the composite with C1018 carbon steel and brass were very similar and higher than the other two metals but the relatively small error bar with brass should be taken to imply that the results were more consistent among repeated testing. The polymer-Inconel system showed good consistently repeated values based on a small error and had the lowest average CoF. The average sample wear rate was highest with Inconel and C1018 carbon steel. In contrast, the polymer-brass system had the lowest sample wear rate due to the soft nature of the metal. Washer wear rate was the most inconsistent measurement in the testing but generally thought to be the lowest with

C1018. The polymer-316SS system was in the middle in terms of all three metrics and in the consistency of their results.

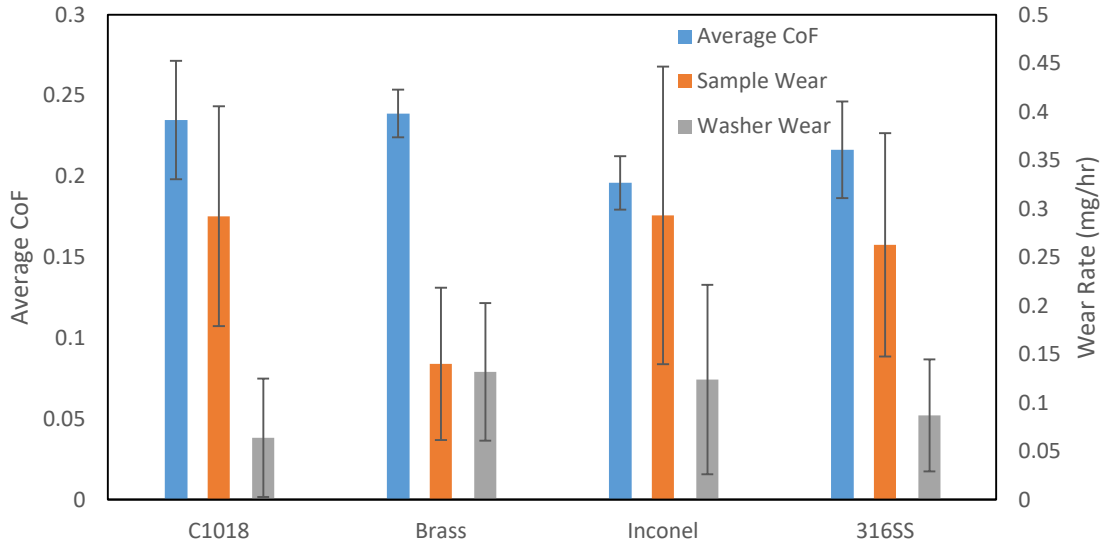


Figure 10 - Average results for each polymer-metal tribology system.

The surface roughness (R_a) of the polymer samples after testing is shown in Figure 11 below. In all cases the average polymer sample surface roughness decreased from the initial state. The same is true for the metal washers (which includes the transfer film) after the tests as seen in Figure 12. The surface roughness was measured for both along the wear track and across the wear track. Both R_a values along and across the wear track are lower than the unworn washers. The R_a along the wear track is lowest as this would be the preferred direction of deposition for the transfer film. The R_a value across the wear track measure both the roughness of the transfer film and boundary region between the worn and unworn sections of the metal washer. There was no relationship between averaged friction results (presented in Figure 10) and initial surface roughness but there was a weakly positive correlation with worn washer surface roughness, in both directions.

The polymer sample surface and transfer film will be examined in more detail for each metal counterface in the following sections below.

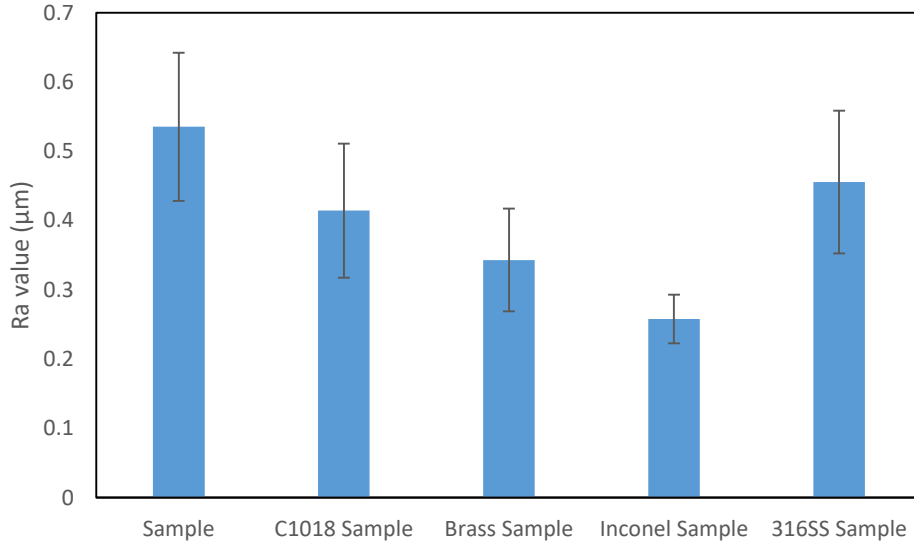


Figure 11 - Surface roughness values of unworn polymer sample compared to worn polymer samples for each polymer-metal system.

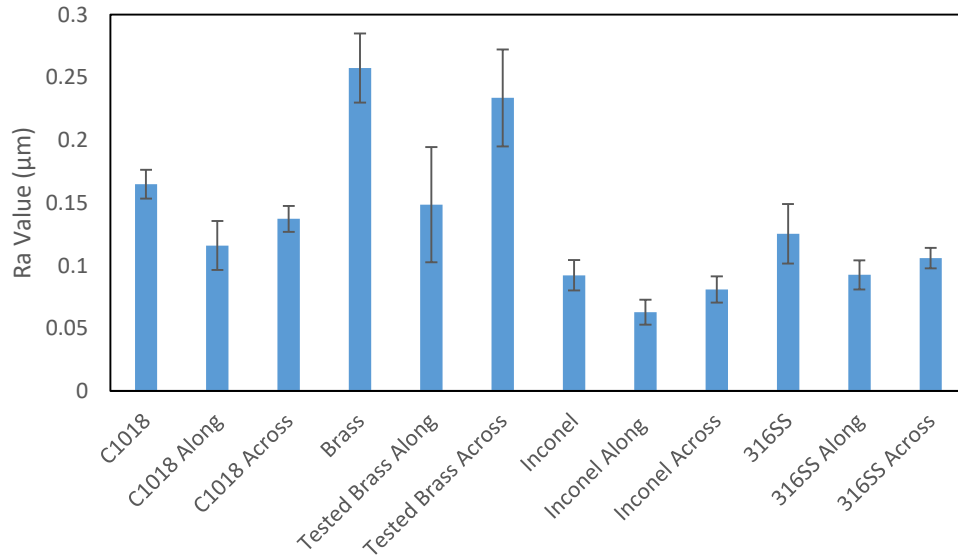


Figure 12 - Surface roughness of unworn metal washers compared to worn metal washers along and across the wear track.

4.3 Carbon Steel C1018 Results

The typical trace for coefficient of friction and temperature curve for a stable and unstable test is shown in Figure 13. Many of the polymer-metal systems in this study produced unstable friction measurement conditions, which merited detailed study to understand the differences in how PTFE was transferred and how the properties of the metal could be causing such differences. For the stable test results in the figure, the measured temperature reached a steady state temperature between 41°C and 43°C whereas in the unstable test, it initially plateaued at 39°C and after 1.5 hrs suddenly started heating up to 51°C.

Stable and unstable test runs with the C1018 washer resulted in similar average CoF, sample wear and washer wear (seen in Figure 14 below) but the stable tribology tests produced a smaller range of average CoF values and only accounts for 25% of the tests performed. However it is important to recognize that the CoF at the end of the test could be much different than the reported averaged result; in the case of Figure 10, the stable condition was operating at a CoF of approximately 0.25 while the unstable condition was much higher at 0.41. It is also important to note that only under unstable behaviour did the washer wear rate reached negative values. A negative washer wear rate implies that the mass of the adhered transfer film is greater than the mass of the washer surface that may have been abrasively worn away.

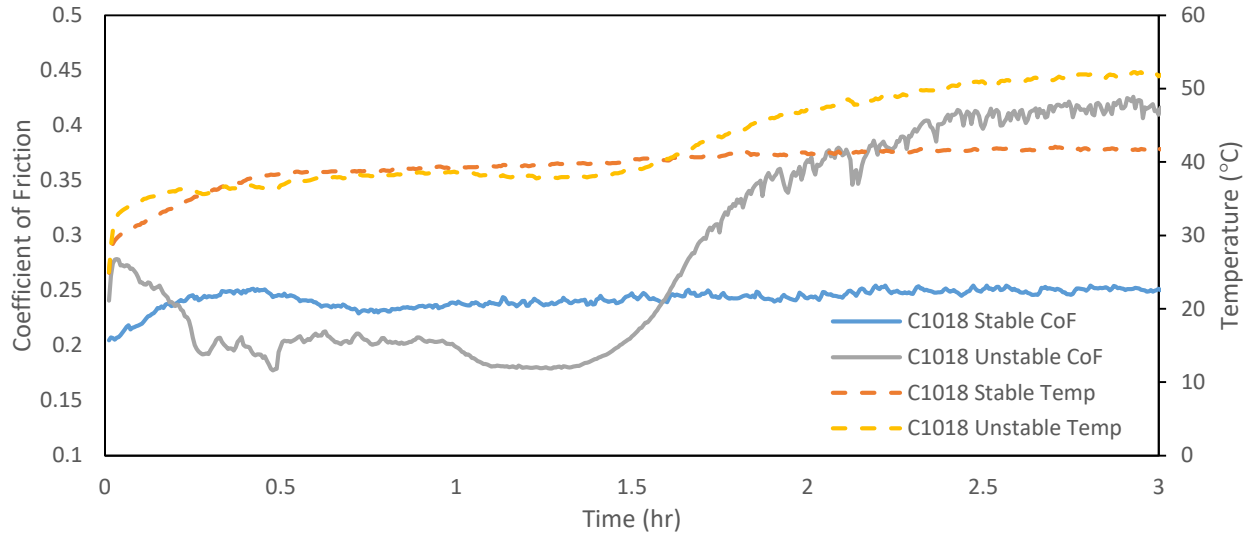


Figure 13 - Typical CoF and temperature curve of stable and unstable C1018 tests.

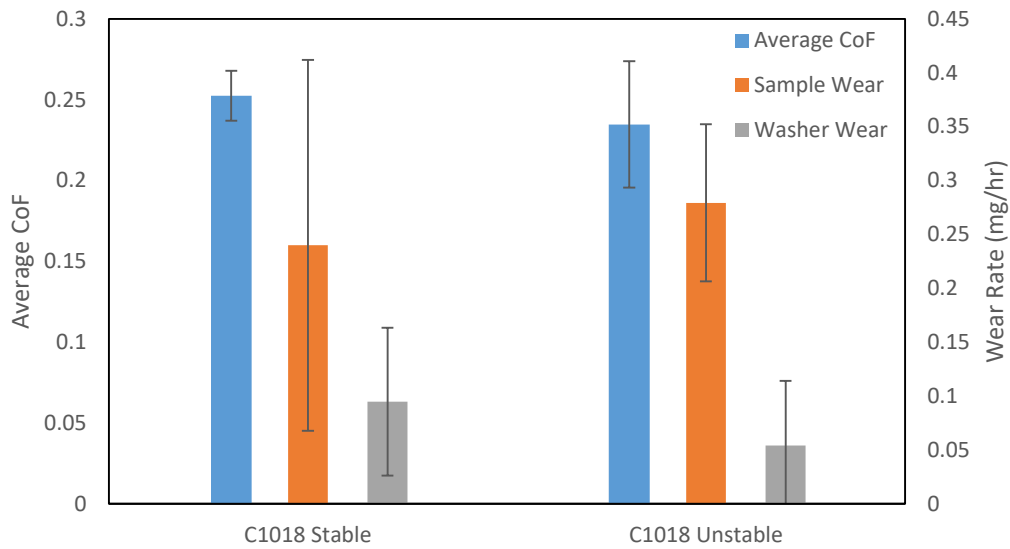


Figure 14 - Average results of stable and unstable C1018 system tests.

Figure 15 demonstrates the difference in polymer surface morphology at the end of a test for the stable and unstable conditions. Under stable conditions, the surface had higher number of large domains of PTFE than by unstable conditions. This is seen in Figure 15(b) where the area distribution shows domains up to the order of $100,000 \mu\text{m}^2$ were present. The domain size and its area distribution from unstable wear were similar to that of the unworn sample but still had some

larger agglomeration of PTFE domains up to $5,000 \mu\text{m}^2$. The PTFE coverage over the polymer sample's surface in both conditions was higher than the unworn sample, though the stable condition had a higher coverage with $16.34\% \pm 3.53\%$ than the unstable condition with $12.90\% \pm 1.72\%$. The transfer film composition on the metal counterface had the opposite trend regarding its distribution of PTFE. From Figure 16, the transfer film produced under unstable conditions had a higher average composition of 39.98 wt% PTFE compared to 24.80 wt% of the stable condition. The opposing trends observed between the surfaces of the stable and unstable conditions suggests that polymer surface morphology is playing a more dominant role in affecting the CoF. A higher number of larger domains, especially those on the order of $2,500 \mu\text{m}^2$, looks to be characteristic of a stable test samples.

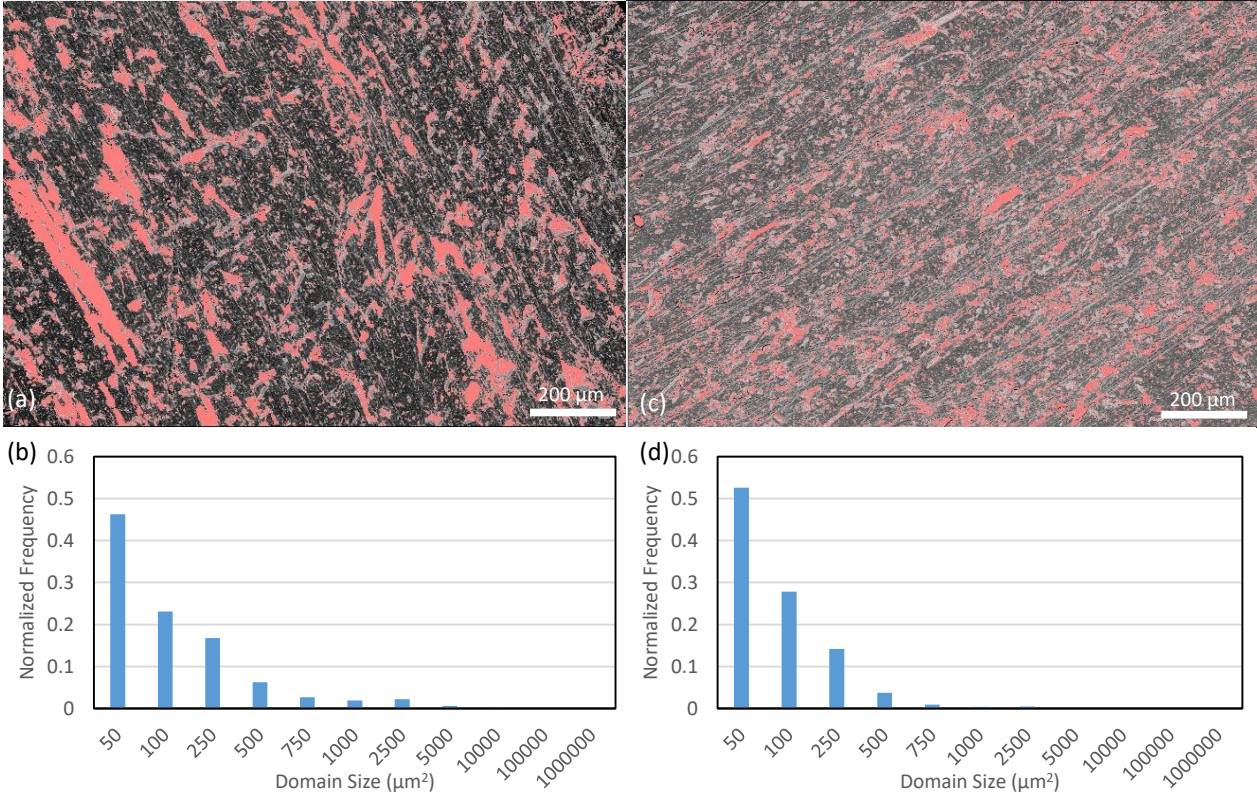


Figure 15 - (a) SEM backscatter electron composition image of C1018 polymer sample surface under stable conditions with PTFE domains highlighted in red and (b) the associated normalized size distribution from 50 μm² to 1,000,000 μm² of C1018 polymer sample surface under stable conditions. (c) SEM backscatter electron composition image of C1018 polymer sample surface under unstable conditions with PTFE domains highlighted in red and (d) the associated normalized size distribution from 50 μm² to 1,000,000 μm² of C1018 polymer sample surface under unstable conditions.

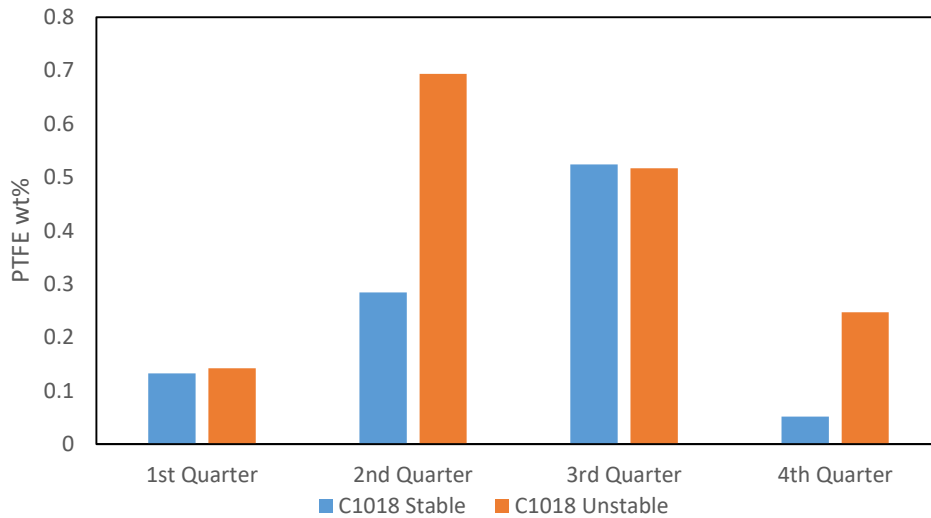


Figure 16 – Comparison of transfer film composition on C1018 washer between a stable and unstable sample. 1st quarter is the inner circumferential quarter while the 4th quarter is the outer circumferential quarter.

4.4 Brass Results

The typical CoF and temperature curves of a stable test for the polymer-brass system, seen below in Figure 17, were similar to those of a stable C1018 test where the CoF and temperature increased initially and then plateaued. The unstable curve however is different; the CoF increased and then changed to steeply decreasing in value while the temperature was very similar to the stable case. Both cases resulted in the same final temperature despite the difference in CoF curve; this similarity in temperature was consistently found in all other tests and always ending between 41.5°C and 43.5°C. This suggests that thermal effects had a less dominant role in the wear behaviour for this system. Moreover, the average CoF shown in Figure 17 was very similar between the stable and unstable test, resulting in values of 0.244 and 0.249 respectively. The stable condition was the most common to occur, far more so than compared to the other metal systems with over 70% of tests performed being stable. From Figure 18, both stable and unstable conditions yielded very similar average CoF values and washer wear rates while the sample wear rate is much higher and less consistent for the stable tests than the unstable tests.

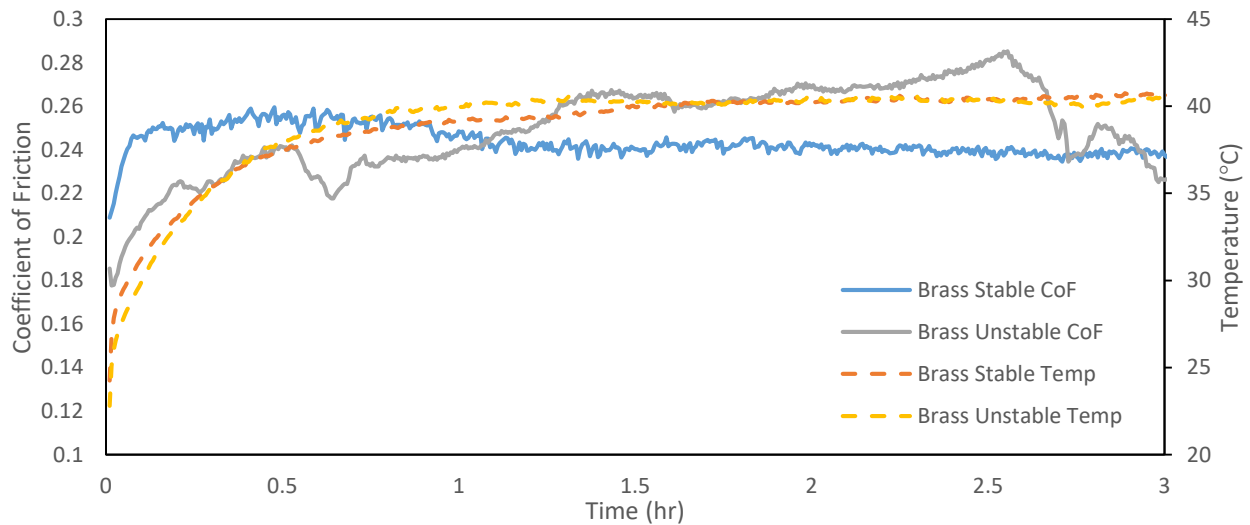


Figure 17 - Typical CoF and temperature curve of stable and unstable brass tests.

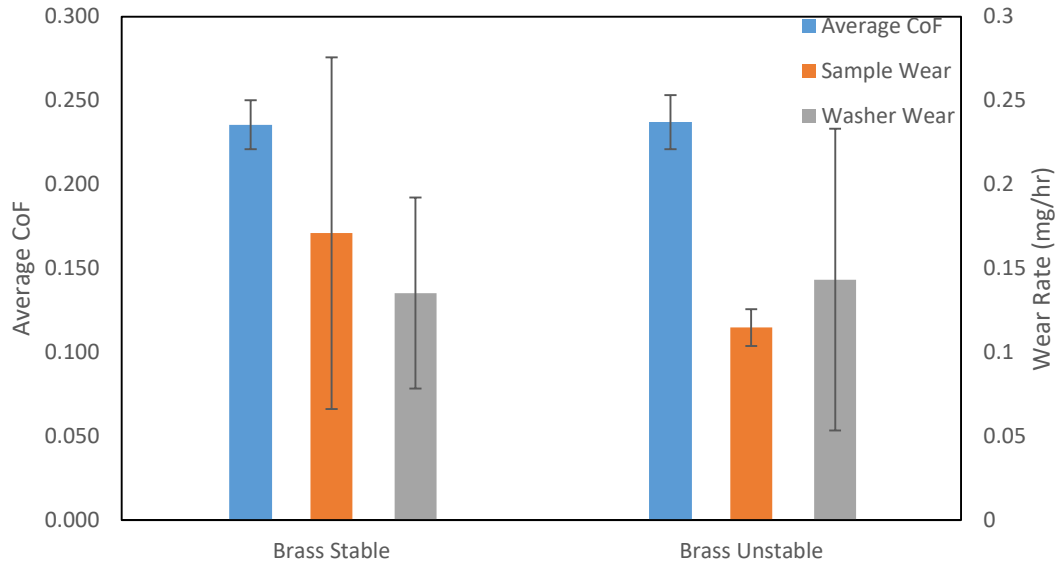


Figure 18 - Average results of stable and unstable brass system tests.

The polymer surface for both cases is shown by SEM in Figure 19. There was very little difference in the surface PTFE coverage at the end of a test run, being $28.93\% \pm 2.58\%$ and $32.85\% \pm 9.66\%$ for stable and unstable conditions, respectively. The only obvious difference was in the domain size distribution where there was a larger increase in the $2500 \mu\text{m}^2$ domains for the stable test which as previously mentioned is characteristic of a stable test sample. Compared to the unworn sample, the PTFE domains had enough mobility to agglomerate into large domains on the surface. The polymer-brass system as a whole had a consistently higher average surface coverage and larger PTFE agglomerates compared to all other metal systems tested in this study. The transfer film distribution, shown in Figure 20, is more evenly distributed compared to the C1018 base case (Figure 16), and the stable condition had a higher average PTFE composition, 28.92wt%, than the unstable condition, 21.82wt%. The analysis of both surfaces indicated that wear stability was achieved when both surfaces became PTFE rich.

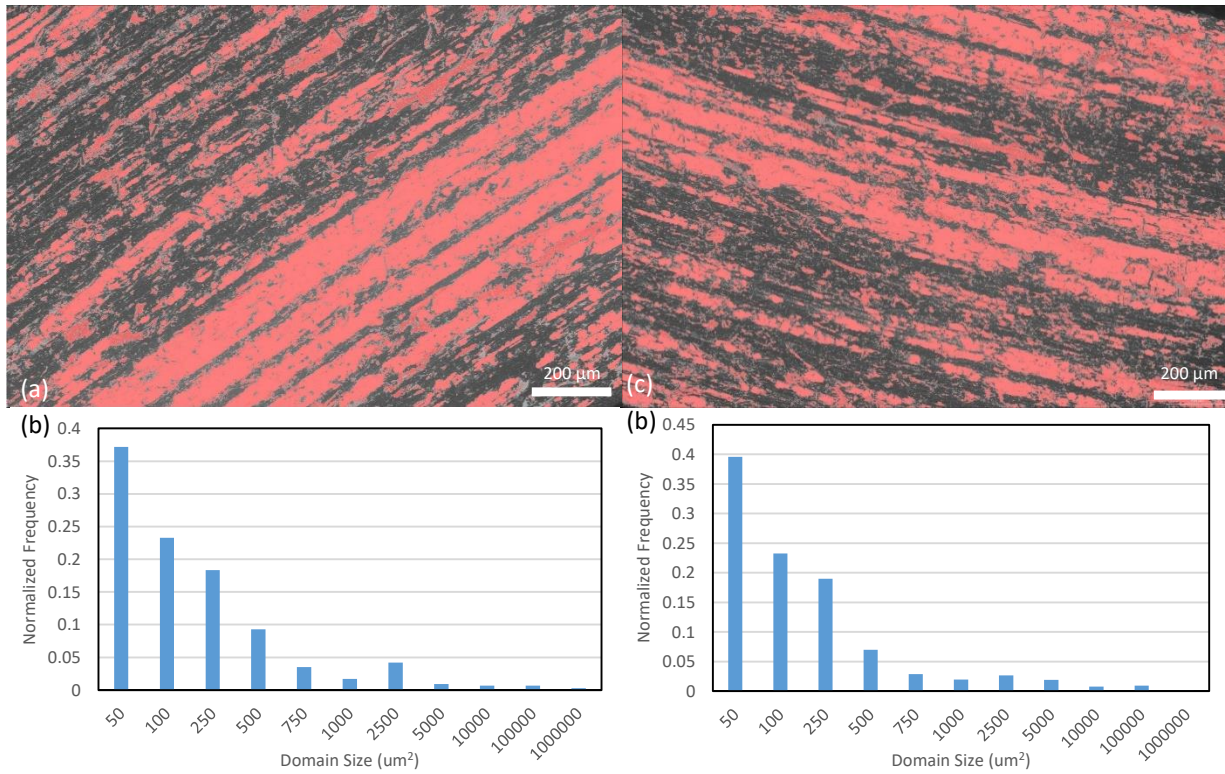


Figure 19 - (a) SEM backscatter electron composition image of brass polymer sample surface under stable conditions with PTFE domains highlighted in red and (b) the associated normalized size distribution from 50 μm² to 1,000,000 μm². (c) SEM backscatter electron composition image of brass polymer sample surface under unstable conditions with PTFE domains highlighted in red and (d) the associated normalized size distribution from 50 μm² to 1,000,000 μm².

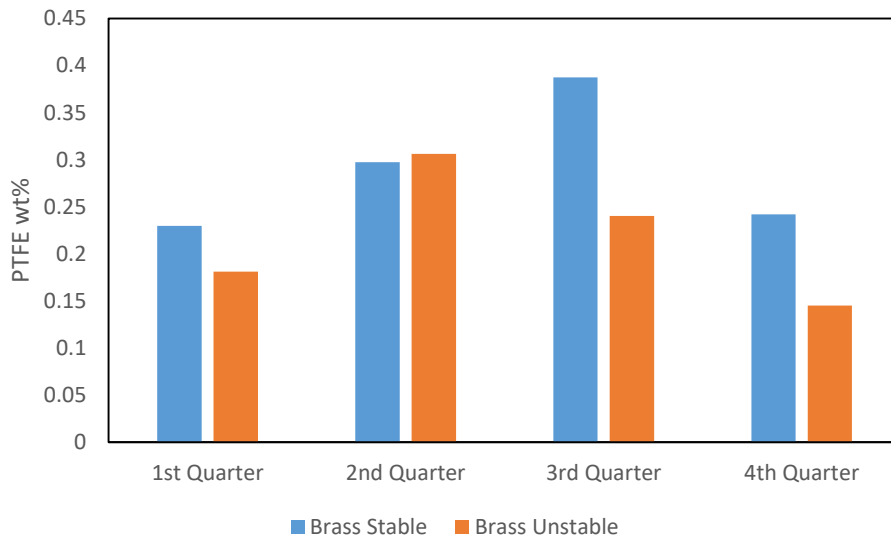


Figure 20 - Comparison of transfer film composition on brass washer between a stable and unstable sample.

4.5 Inconel Results

The CoF and temperature curves of a typical stable and unstable test for the polymer-Inconel system are shown below in Figure 21. Compared with the stable case of the polymer-C1018 system, a stable condition with Inconel produced a similar looking CoF curve shape but yielded a lower stabilized and average CoF value of 0.196. Despite having a lower CoF value, the indicated temperature was higher than the stable C1018 system due to the lower thermal conductivity of Inconel which meant that less heat was dissipated. The unstable condition showed a much more cyclic pattern for CoF with peaks and valleys that seen for C1018 or brass. Depending on the amplitude and the frequency of the oscillations, the average CoF value can be higher or similar to the stable case; the average CoF value for the unstable test presented below was 0.232 but some unstable tests exhibited an average CoF value below 0.19. The temperature curve follows the CoF trend with an approximately 60 s lag, suggesting that the change in CoF preceded the change in temperature. Figure 22 below summarizes the averaged results of the stable and unstable tests. The stable tests had a higher average CoF value and sample wear rate whereas unstable tests had a higher washer wear rate; this proposes that the cause for instability is linked with improper loading, commonly called edge loading, of the sample against the washer. The relatively high sample wear rate indicates the lack of adhesion between the transfer film and washer surface as the transfer film is supposed to act as a protective layer against the hard asperities of the Inconel surface to reduce wear rate.

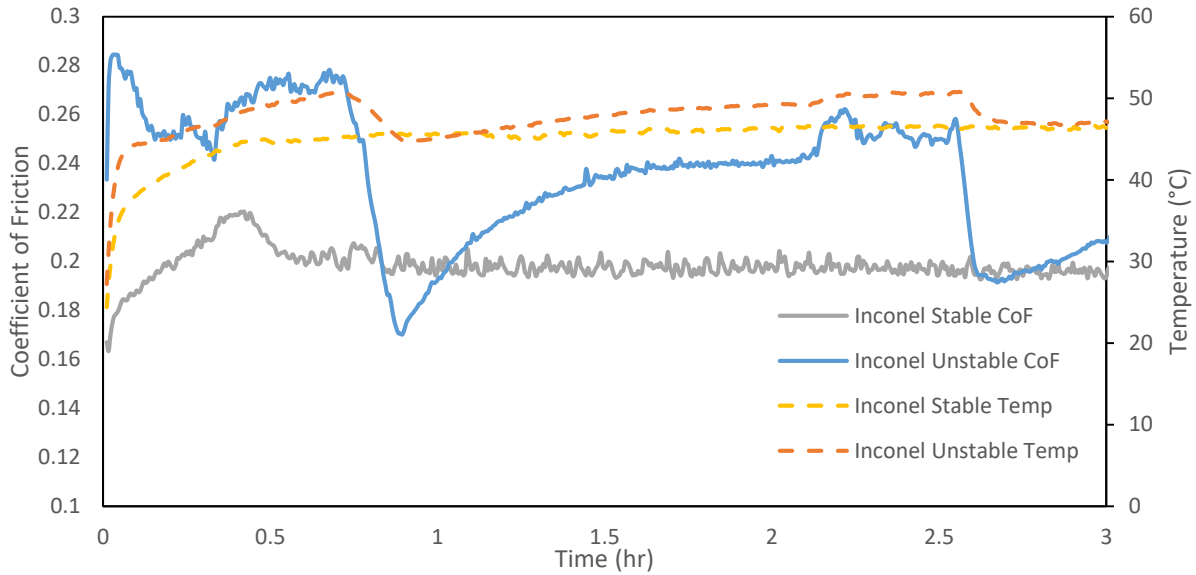


Figure 21 - Typical CoF and temperature curve of stable and unstable Inconel tests.

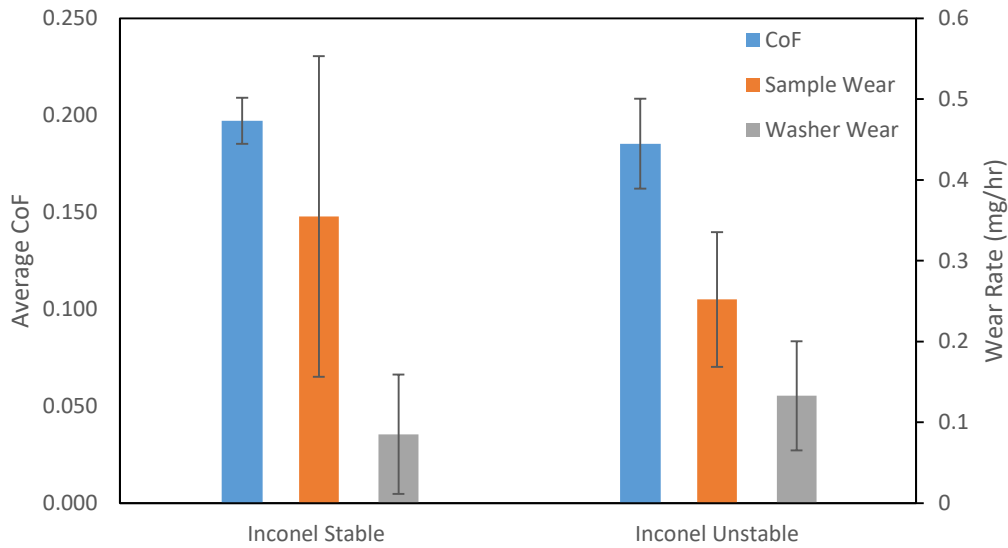


Figure 22 - Average results of stable and unstable Inconel system tests.

To better understand the behaviour of this system, the polymer surface was analyzed by SEM for a stable test and for an unstable test, specifically examined when the CoF curve exhibited a peak and then when it showed a valley; the consistency of peaks and valleys made this analysis possible whereas for the C1018 or brass, there was no ability to predict when to stop the test.

Interestingly, Figure 23(a) shows little difference in PTFE distribution for the stable condition from the unworn polymer surface shown in Figure 8. The PTFE domain sizes were slightly larger and the carbon fibers were now seen to be oriented in the sliding direction on the polymer surface. The domain size distribution in Figure 23(b) supports that there was little change in domain size for the stable condition with an increase in frequency of the $50\mu\text{m}^2$ domains. The surface coverage decreased from the original unworn sample of 9.19% to $5.30\% \pm 1.35\%$. Figure 24(a) shows the polymer surface examined at a peak in the CoF curve under unstable testing condition. There is now seen to be some agglomeration of the PTFE domains, which is represented in Figure 24(c) by the increased skewness seen in the distribution and agglomerated domains reaching up to $10,000\mu\text{m}^2$. The polymer surface examined at a point in the test when a valley in the CoF curve existed, is shown in Figure 24(c). The surface was similar to the surface corresponding to the peak, at least in regards to agglomerating being significantly present. However, the PTFE domain sizes were larger and almost forms a continuous streak close to the outer edge. The distribution in Figure 24(d) shows that the maximum domain size was now on the order of $100,000\mu\text{m}^2$. The surface coverage of PTFE at the peak and valley was $10.57\% \pm 3.37\%$ and $15.43\% \pm 3.09\%$, respectively indicating that more PTFE was at the polymer surface while the CoF was lower.

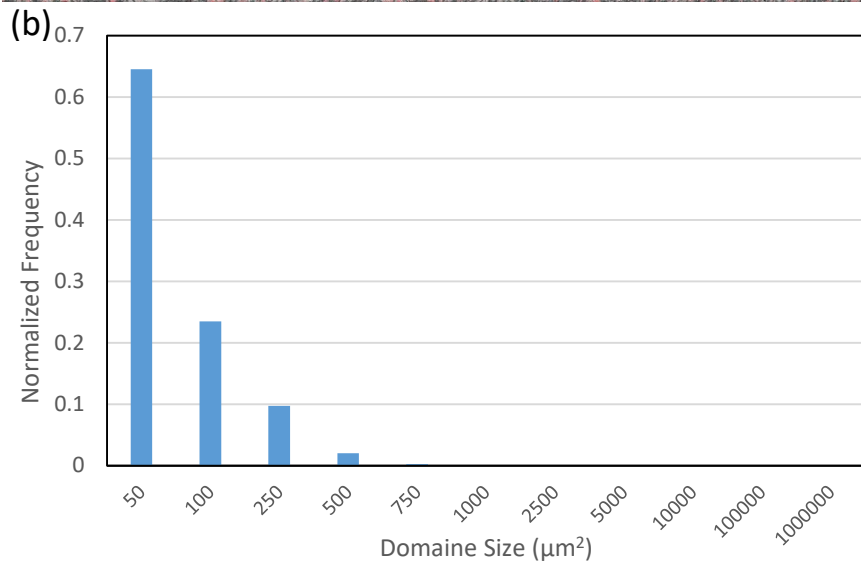
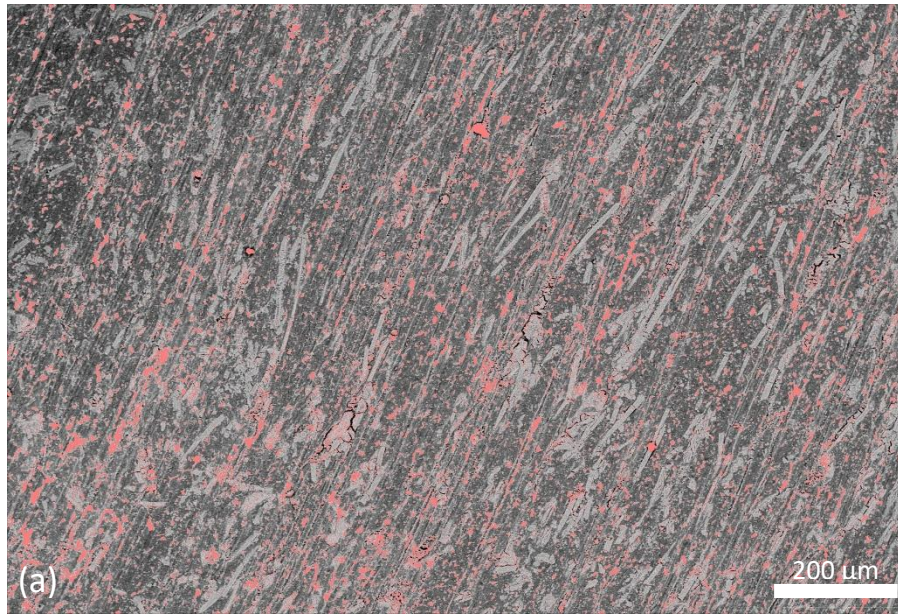


Figure 23 - (a) SEM backscatter electron composition image of Inconel polymer sample surface under stable conditions with PTFE domains highlighted in red and (b) the associated normalized size distribution from 50 μm^2 to 1,000,000 μm^2 .

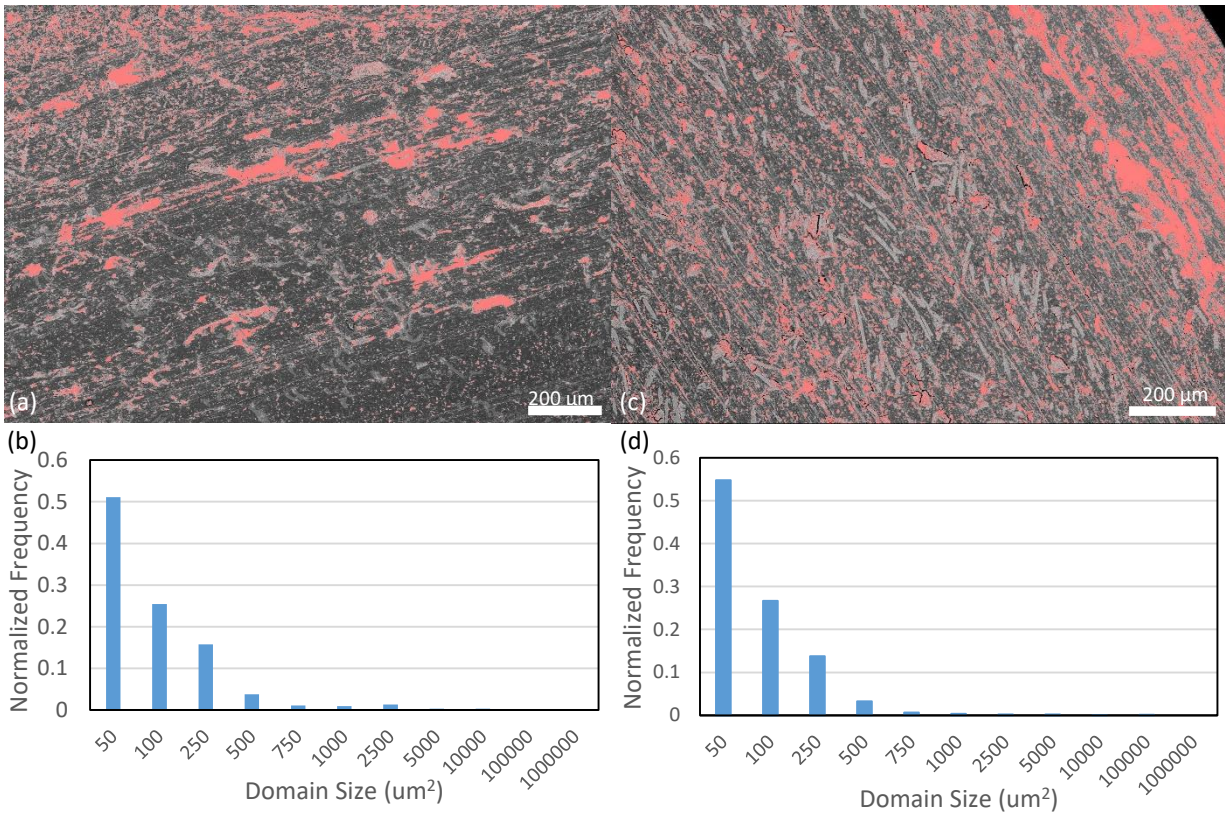


Figure 24 - (a) SEM backscatter electron composition image of Inconel polymer sample surface under unstable conditions at the peak CoF value with PTFE domains highlighted in red and (b) the associated normalized size distribution from $50 \mu\text{m}^2$ to $1,000,000 \mu\text{m}^2$. (c) SEM backscatter electron composition image of Inconel polymer sample surface under unstable conditions at the valley CoF value with PTFE domains highlighted in red and (d) the associated normalized size distribution from $50 \mu\text{m}^2$ to $1,000,000 \mu\text{m}^2$.

Composition of the transfer film around the surface of the washer is shown in Figure 25 with a uniform dispersion of PTFE for the stable test conditions, whereas heterogeneity was seen by large localized amounts of PTFE being present in both unstable conditions. Similar to the previously discussed polymer-metal systems, a relatively uniform transfer film composition profile is characteristic of a stable test. The average transfer film composition for the stable test, and peak and valley of the unstable test was 20.42wt%, 20.13wt% and 23.80wt%, respectively. A possible reason for the stable and peak case having very similar average composition value was that they both ended at a similar CoF value of 0.2 whereas in the valley case the test ended at 0.16.

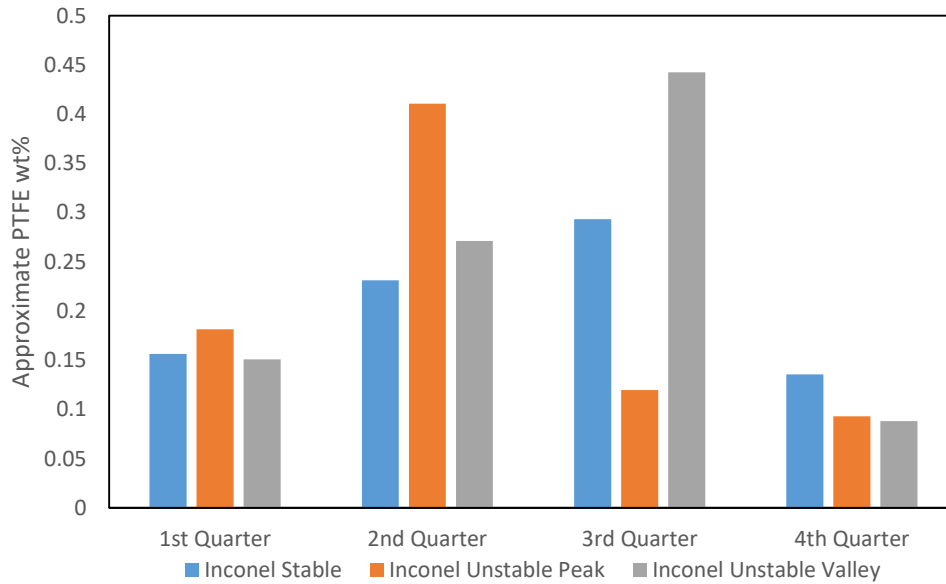


Figure 25- Comparison of transfer film composition on Inconel washer between a stable and unstable sample at the peak and valley positions of the CoF curve.

4.6 Stainless Steel 316SS Results

The polymer-316SS system produced the most unstable CoF curves of all metals tested. Figure 26 below demonstrates that before the CoF stabilized in the ‘stable condition’ there was a large dip before rising back to a stabilized value that it oscillates around. In some tests, this was a more gradual and flatter curve but took long to stabilize. The unstable condition featured a more erratic performance where the system was at a low CoF regime for approximately an hour after the initial break-in period and then rose to a high CoF regime for approximately an hour before decreasing again. Within both regimes, the CoF curve oscillates erratically. The temperature curves corresponding with these CoF curves showed no noticeable inconsistencies to explain the variability in CoF. However, the recorded operating temperatures were generally highest compared to the other metal systems discussed. The summary of averaged test results, presented in Figure 27 below, for both stable and unstable tests, are very similar. The only notable difference is the

average sample wear rate for the stable condition was slightly higher. From the data presented so far there is no clear cause for the system to perform in a stable or unstable manner.

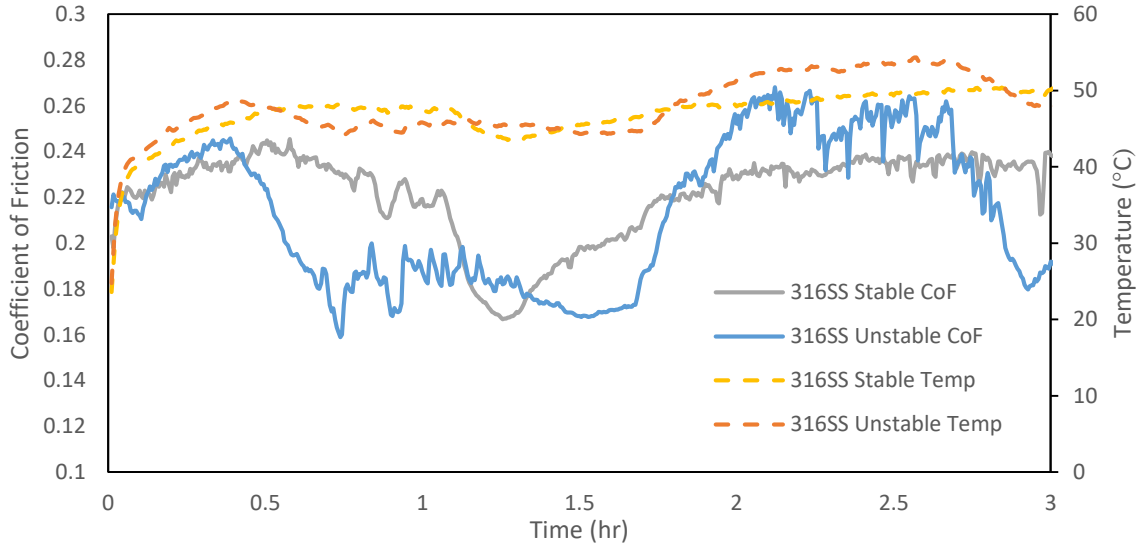


Figure 26 - Typical CoF and temperature curve of stable and unstable 316SS tests.

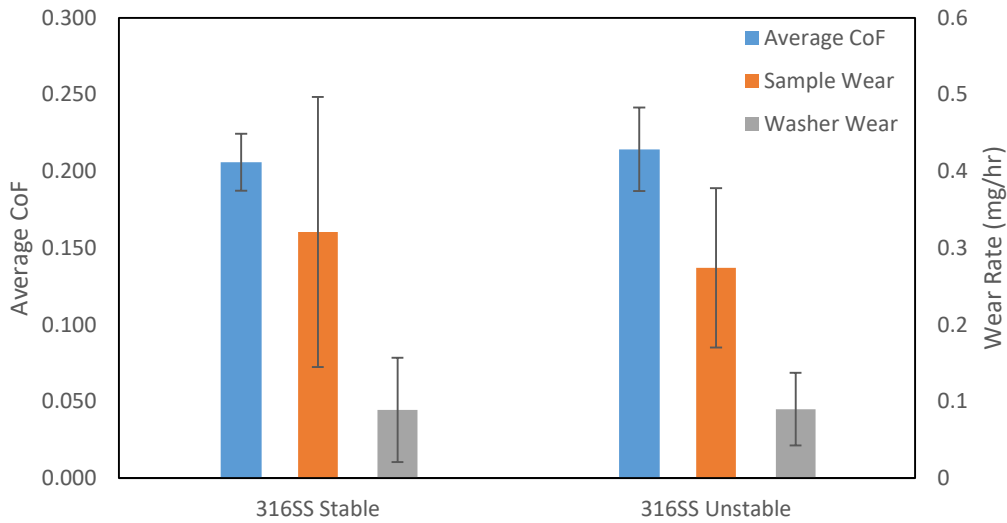


Figure 27 - Average results of stable and unstable 316SS system tests.

Upon inspection of the polymer surfaces, there were some differences in the domain size between the unstable and stable conditions. Figure 28(a) shows that for a stable condition there were PTFE agglomeration on the surface with the largest domain size on the order of 10,000 μm^2 .

Most of the PTFE domains were spread across the surface with some clustering on the outer edge. In comparison, the polymer surface of an unstable test, shown in Figure 28(c), more closely resembles the surface of the unstable C1018 baseline system presented in Figure 15(c). There was minor agglomeration of PTFE and the domains were evenly spread throughout. The largest PTFE domain size was on the order of $2,500 \mu\text{m}^2$, lower in number and smaller than the stable polymer surface. The PTFE surface coverage of the stable and unstable case was $11.03\% \pm 0.76\%$ and $8.58\% \pm 1.57\%$, respectively. This follows the trend of C1018 and brass where the stable test had a higher surface coverage, larger domain sizes on the polymer surface and a higher number of $2,500 \mu\text{m}^2$ domains.

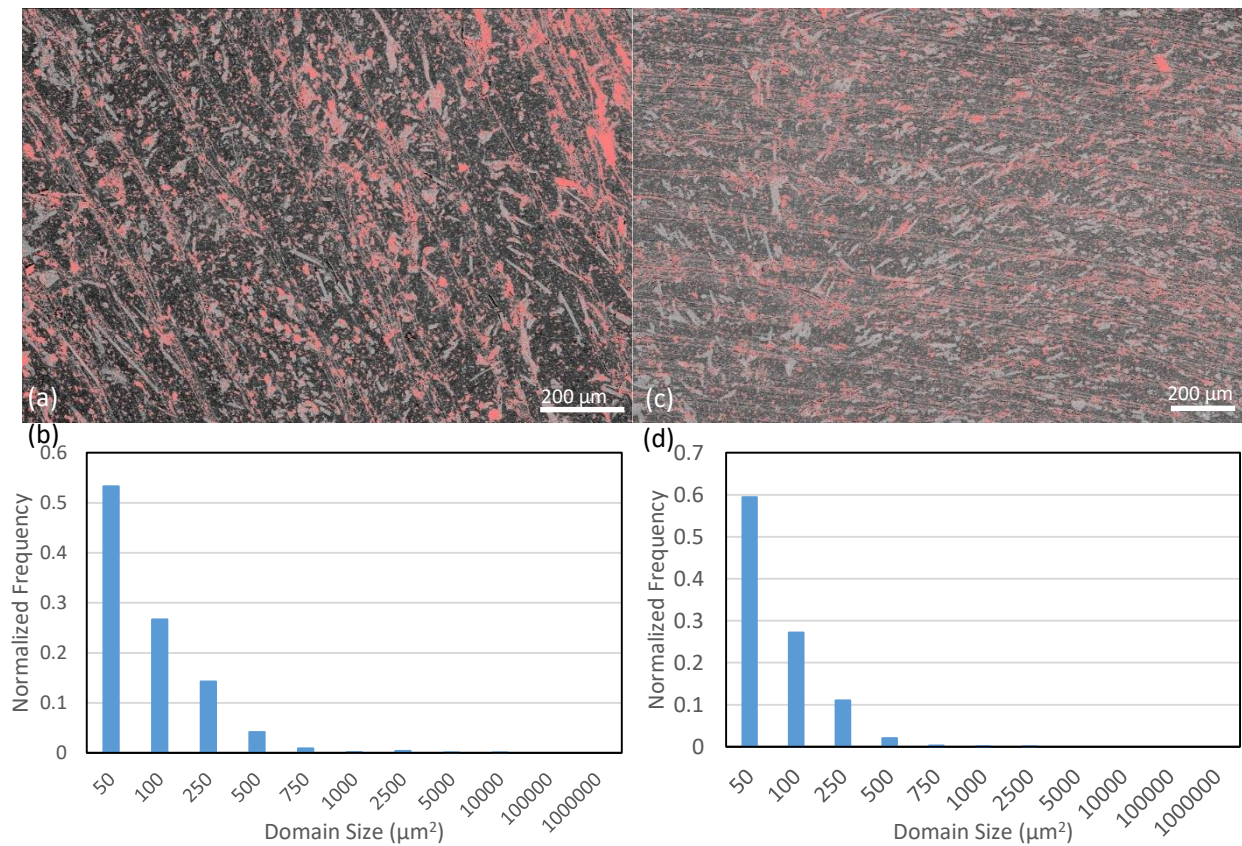


Figure 28 - a) SEM backscatter electron composition image of 316SS polymer sample surface under stable conditions with PTFE domains highlighted in red and (b) the associated normalized size distribution from $50 \mu\text{m}^2$ to $1,000,000 \mu\text{m}^2$. (c) SEM backscatter electron composition image of 316SS polymer sample surface under unstable conditions with PTFE domains highlighted in red and (d) the associated normalized size distribution from $50 \mu\text{m}^2$ to $1,000,000 \mu\text{m}^2$.

The transfer film composition presented in Figure 29 revealed two different profiles. The stable case had a sharper profile where there was a high concentration of PTFE in the middle and low concentration on the outer edges, whereas the unstable case featured a more uniform deposition profile on the washer surface. This contradicts the trend set by the previously discussed metal systems where the stable case had a more uniform profile. The average film composition was 49.01wt% and 48.37wt% PTFE, respectively for the stable and unstable cases. With such a small difference between the two average film compositions, it appears that the polymer surface morphology was the dominant factor affecting the stability and performance of the polymer-316SS system.

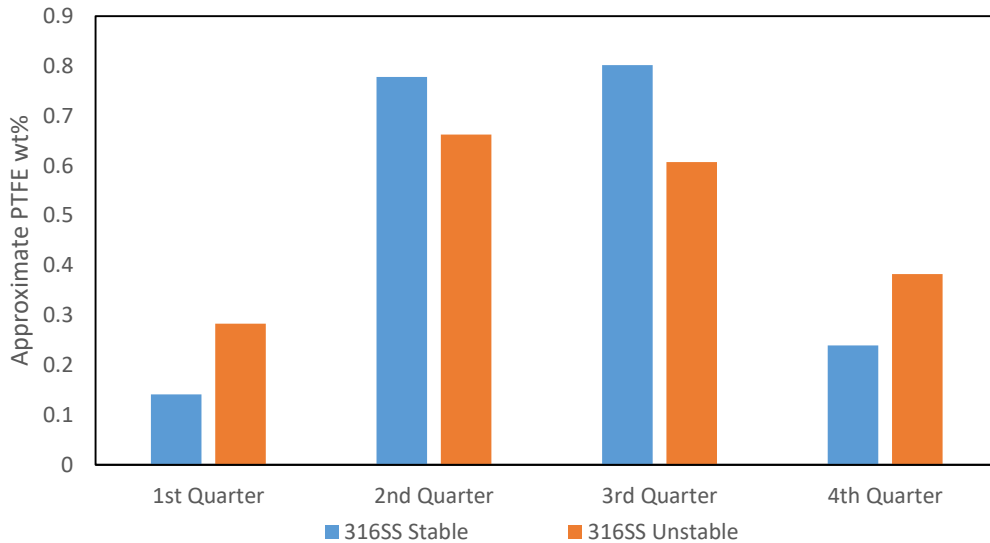


Figure 29 - Comparison of transfer film composition on 316SS washer between a stable and unstable sample.

Chapter 5 Discussion

5.1 Condition for stability

For stable performance, the systems appeared to require that the polymer transfer film be thick, uniform and strongly adhered to their metal counterfaces, in order to provide a smooth surface for the polymer to wear on and protect it from the asperities on the metal surface. Although mechanical interlocking and electrostatic attraction between polymer chains and the porous, rough surface of the metals can be strong, tribochemical interactions can either further strengthen or weaken the adhesion of the transfer film. The activation energy required for adhesion is supplied by the thermal energy generated during the friction process. Tzanakis et al. reported that although the measured operating temperature might be low, the actual flash temperature between the carbon fiber and metal counterface can reach several hundred degrees Celsius and in some cases close to 1000°C (Tzanakis et al. 2013). Evidence that the temperature at the interface at least exceeded the melting point of PTFE can be seen in Figure 30 below where not only did the heat allow the agglomeration of PTFE domains but also allowed the carbon fibers in the polymer sample to become oriented in the direction of sliding. Using this thermal energy source, tribochemical reactions can occur at the interface during the friction process.

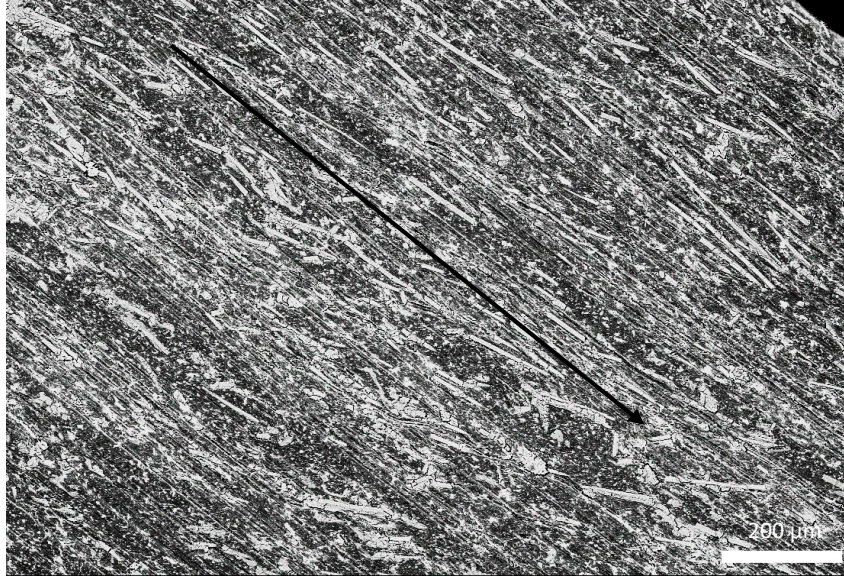


Figure 30 - Fiber reorientation under friction and wear with arrow indicating direction of sliding.

The tribochemical reactions between the polymer transfer film and metal surface are complex and often difficult to observe with conventional analysis techniques. In recent years, some progress has been made to explain the tribochemistry behind the adhesion of transfer films. Most studies focus on PTFE, due to the low activation energy for slippage between crystalline slices, ease of transfer to occur, and its effectiveness as a solid lubricant, but is applicable to other polymers as well (Tanaka et al. 1973). By understanding the reaction mechanism and how it is activated, it is possible to explain why the friction and wear behaviour differs between metal surfaces. During the initial stages of friction when there is very little built up thermal energy, most of the metal oxide layer is abrasively worn away by the polymer exposing a polished fresh metal surface (Eiss & Potter 1985). If any transfer film is attached to the metal surface at this point, it is due to the aforementioned mechanical interlocking and electrostatic attraction. As thermal energy is built up at the interface, due to the insulating nature of polymers, a few mechanisms can be activated. First of all, under the intense heat new metal oxides can form in small amounts where it is safely isolated from the abrasive forces. Fatigue can occur on the polymer surface generating radicals that can break polymer chains or react with the atmosphere (Jintang 2000). Any peroxide

radicals generated during this process can also affect the metal surface and any already adhered transfer film. This is when tribochemical reactions, shown below in Figure 31, start to occur. Chain scission of the polymer backbone can occur and any carbon double bond can be broken but more interestingly bonds between the backbone and side groups can also be broken (Jintang 2000; Onodera et al. 2014). Any fragments containing a radical now has the possibility to react with metal oxides, fresh metal surface and nitrogen, oxygen and water from the atmosphere (Onodera et al. 2014). Metal oxides (MO) and ions can attach itself to the radical containing site of a polymer backbone or a detached side group (Jintang 2000). Between reactions with water, nitrogen and oxygen from the atmosphere, the activation energy is lower with water and is therefore the more dominant reaction to occur (Onodera et al. 2014). The reaction between water and the polymer chain can yield hydroxyl, carbonyl and carboxyl groups to be attached to the polymer chain. Onodera et al. used molecular dynamics (MD) and quantum chemical molecular dynamics (QCMD) simulations to show that carboxyl groups allowed a thicker transfer film to be formed between pure PTFE and an aluminum surface (Onodera et al. 2014). This is due to the increased adhesion from electrostatic attraction between the transfer film and metal surface. Other side products are also formed during the reactions. Metal fluoride (MF) and hydrogen fluoride (HF) can be formed from any detached fluorine ions or the fluorine can directly fluorinate the metal surface (Jintang 2000; Onodera et al. 2014). Since HF is highly reactive, it will most likely help further fluorinate the metal surface. Any fluorine attached to the metal surface will decrease transfer film thickness and adhesion due to the increased electrostatic repulsion. Despite that, Onodera et al. also reported through their simulations that the hydrogen in the carboxyl group can be electrostatically attracted to any fluorine attached to the metal surface (Onodera et al. 2014). Hydroxyl groups can also attach to the metal surface and/or polymer chain thus increasing

hydrogen bonding between the two. Evidence of these reactions was seen by the EDS analysis as high levels of oxygen and fluorine were detected. In some cases, the oxygen detected by EDS exceeded 10 wt% during analysis and the fluorine to carbon weight ratio far exceeded the theoretical limit of 100% PTFE. For such high levels to be detected, oxygen and fluorine must have reacted with the metal surface. With increased adhesion a thicker transfer film can be securely attached to the metal surface amidst wear forces.

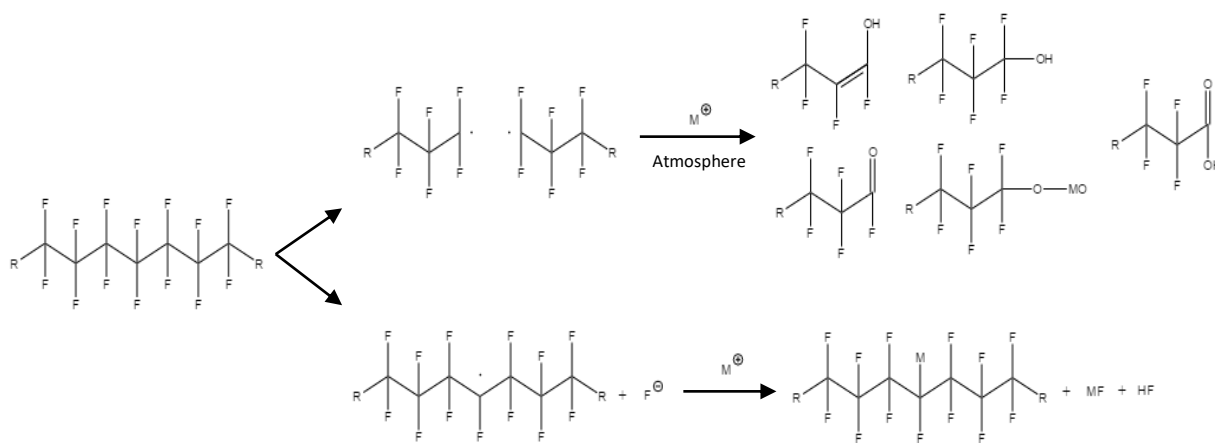


Figure 31 - Proposed tribochemical reaction mechanism between polymer and metal adapted from Jintang and Onodera et al (Jintang 2000; Onodera et al. 2014). PTFE was used as an example for its ease of transfer and simplicity.

5.2 Carbon Steel C1018 System

In order for the above lubricating mechanism based on transfer film adhesion to work well the metal counterface must be relatively reactive, if not adherence must rely upon electrostatic attraction and mechanical interlocking. Carbon steel C1018 has up to 99.26 wt% iron which is the second least reactive metal discussed in this thesis with an electronegativity value of 1.83. This can be seen as the average PTFE composition of the transfer film (39.98 wt%) on this metal surface is lower than the more reactive stainless steel and higher than the less reactive Inconel. It is also the polymer-metal system that was least likely to be stable, with only 25% of the tests performed being stable and experiencing a relatively high sample wear rate. Another possible reason for the

high chance of instability and wear rate is heat buildup. Despite being the best thermal conductor out of the four metals, temperature is evidently a dominant factor in causing instability. From the characteristic unstable curve show in Figure 32 below, the system plateaued at 39°C for a while before destabilizing to higher temperatures and yielding a higher CoF. The exact reason for this is not known but it is apparent that the transfer film is being disrupted and possibly worn away. Without a uniform transfer film, the friction will not stabilize and the polymer is not protected from the asperities of the metal surface.

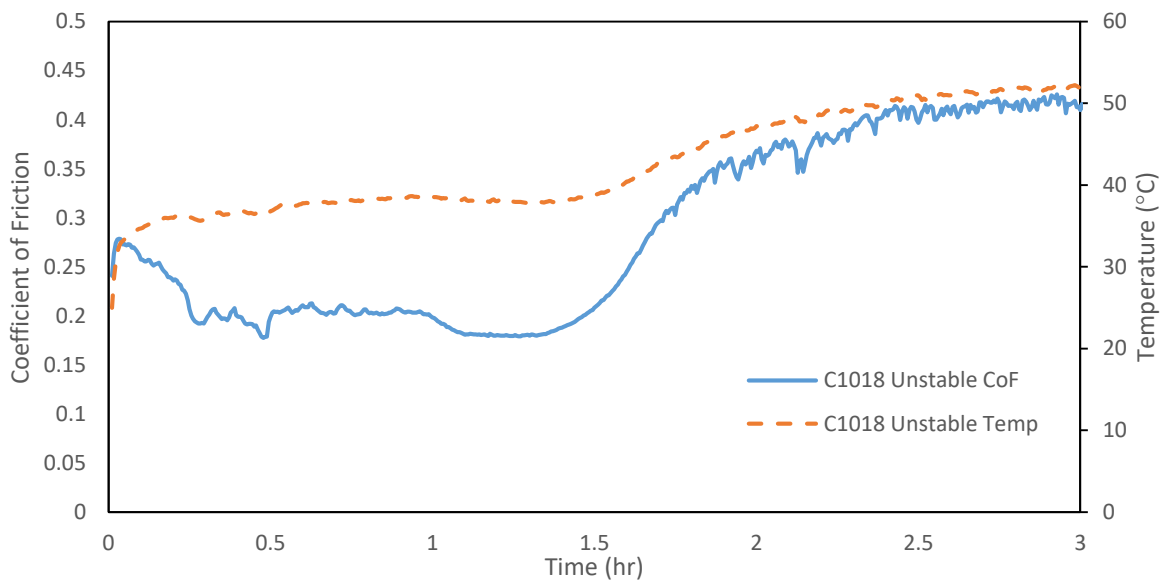


Figure 32 - CoF and temperature curve of an unstable C1018 test.

5.3 Brass System

Although copper is relatively unreactive, the polymer-brass system has the highest percentage of stable tests (70%) and the lowest sample wear rates, which was attributed to the reactivity of zinc of which accounts for 40 wt% of brass. Amongst all the metals used in the alloys, zinc is the most reactive with an electronegativity value of 1.65. The reactivity of zinc can be seen by the high PTFE coverage (28.93%) and large domains on the polymer surface, which must have

been drawn out from the subsurface regions of the sample. After considering the copper component of brass, which has a relatively high electronegative value of 1.90, the weight average electronegativity value is approximately 1.80. Another reason for good adhesion is the porous structure of brass into which the polymer chains entangle (Halley & Mackay 1994). This is also why brass has a relatively low PTFE content (28.92 wt%) in its transfer film (relative to the carbon steel results), despite being the most reactive, as the polymer matrix will also more easily adhere to the brass surface. In polymer extrusion, brass is known to enable stable flow devoid of melt fracture at higher flow rates. This is due to the dezincification process, where the reactive zinc is removed, at the surfaces leaves a very porous copper structure that allows polymer chains to penetrate and entangle (Halley & Mackay 1994; Person 1997). During friction and wear, the dezincification is not as dominant as it would be in extrusion because during extrusion fresh molten polymer is constantly flowing over the die whereas the testing configuration used in this study has the same polymer rubbing against it for the duration of the test. Since there is a balance of tribochemical reactions and dezincification, brass should provide both strong mechanical interlocking and electrostatic attraction to the transfer film which offer stable frictional performance and low sample wear.

5.4 Stainless Steel 316SS System

Stainless steel 316SS is slightly more reactive than carbon steel C1018 and less reactive than brass when considering the three main metal elements used in its fabrication. Although the majority is still made of iron and nickel, the chromium is relatively reactive with an electronegativity value of 1.66. The weight average electronegativity value when considering just the three main ingredients is approximately 1.81. As a result, this polymer-metal system produced stable tests 50% of the time. It also has the highest average PTFE composition (49.01 wt%) and

fluorine EDS signal in its transfer film. With iron and nickel being relatively stable, chromium will react with the atmosphere and polymer first. The likely reason for this system to produce the most unstable CoF curves is the poor mixing of chromium during manufacturing. During EDS analysis, chromium is not always detected and manually adding it into the list of elements for quantification calculations caused the results to be unreliable. This caused the stainless steel surface to have patches of high and low reactivity which would decrease the uniformity of the transfer film in terms of thickness and composition and thus affect friction and wear performance.

5.5 Inconel System

Inconel is the most stable metal alloy in this study due to its high nickel content. Nickel has an electronegativity value of 1.91 making it slightly more stable than copper. After also considering chromium, molybdenum, iron and niobium, the weight average electronegativity value is 1.86. This is reflected in the PTFE content of the transfer film (20.42%) which is the lowest of the four metal systems. Half of the tests performed (50%) were considered stable which is on par with stainless steel despite being less reactive. The cause for unexpected high number of stable test could be the composition and manufacturing of the alloy. Inconel features metals with the largest spread of electronegativity values. Niobium and chromium has electronegativity values of 1.60 and 1.66 respectively whereas nickel and molybdenum is respectively 1.90 and 2.16. Good mixing of all the ingredients is evidently an issue as one washer produced more stable tests than others. The non-uniformity of metal composition would not be as severe as stainless steel because all elements were consistently detected by EDS. This can also be a possible explanation for the oscillations discussed in the previous section where a washer might have regions of high and low reactivity causing the transfer film to be cyclically worn away and replenished.

Chapter 6 Conclusion

Polymer composites has drawn interest from academia and industry for replacing traditional metal and ceramic parts in tribological applications. Their high strength, processability and chemical resistance makes them an attractive alternative material for both manufacturers and users. To better optimize polymer composites for various tribological applications, the tribochemical effects in the contacting area of polymer-metal systems must be examined.

In this study, a PPE+PS blend based composite filled with carbon fiber, carbon black and PTFE was tested against carbon steel C1018, naval brass 485, stainless steel 316 and Inconel 625, all under the same conditions. This ensured that any differences in the results were due to the dissimilarities in the metals. The tests were conducted with a vertical thrust type tribometer and the surface features of the polymer and metal samples were investigated.

The testing revealed that the tribological performance is indeed affected by the composition of the metal counterface and each polymer-metal system had differences in their tendency to operate in a stable and unstable state. SEM micrographs show agglomeration of PTFE domains and the reorientation of carbon fibers in some instances. The PTFE surface coverage on the polymer sample also differed depending on the metal counterface. Stable tests showed a more uniform transfer film composition across the washer surface and a high number of 2,500 μm^2 domains on the polymer surface. Overall the polymer-brass system showed the most consistent and stable behaviour with the highest PTFE coverage on the polymer sample's surface.

The composition of the metal affects the friction and wear performance of the polymer composite through tribochemical reactions that occur at the interface. A thicker and more uniform transfer film is able to provide a smooth asperity-free surface for the polymer to slide against,

resulting in a stable and low wear operation. In order for a thick transfer film to be strongly adhered, a series of reactions must occur at the interface to increase electrostatic adhesion. The intense buildup of thermal energy provides the required activation energy for these stated reactions. The presence of carboxyl groups was reported in the literature to increase adhesion the most and the reactivity of the interface must be high for more carboxyl groups to attach to the polymer transfer film and metal surface. The reactivity of each metal alloy correlated well with the number of stable tests each polymer-metal system achieved and the surface coverage of PTFE. Distribution of reactive elements in the metal washers and temperature were proposed as causes for instability.

In conclusion, this study has shown that the tribological performance of polymer composites can differ depending on the composition of the counterface material. The friction and wear results of stable and unstable tests of each metal system were compared. Analysis using SEM and EDS were conducted for the surfaces of the polymer and metal to investigate the effect of possible tribochemical reactions on the contacting area. The reactivity of the metal was shown to have a major impact on the performance of the polymer composite.

References

- Bahadur, S., 2000. The development of transfer layers and their role in polymer tribology. *Wear*, 245(1–2), pp.92–99.
- Bahadur, S. & Sunkara, C., 2005. Effect of transfer film structure, composition and bonding on the tribological behavior of polyphenylene sulfide filled with nano particles of TiO₂, ZnO, CuO and SiC. *Wear*, 258(9), pp.1411–1421.
- Brostow, W. et al., 2010. Tribology of polymers and polymer-based composites. *Journal of Materials Education*, 2010(Vol.32 (5-6): 273-290), pp.273–290. Available at: 2010 Tribology of polymers and polymer-based composites_UNT_EDU_.pdf.
- Buckley, D.H., 1981. *Surface effects in adhesion, friction, wear, and lubrication*, Elsevier.
- Chiu, P.Y. et al., 2012. Design of low wear polymer composites. *Tribology Letters*, 45(1), pp.79–87.
- Conte, M. & Igartua, A., 2012. Study of PTFE composites tribological behavior. *Wear*, 296(1–2), pp.568–574. Available at: <http://dx.doi.org/10.1016/j.wear.2012.08.015>.
- Conte, M., Pinedo, B. & Igartua, A., 2013. Role of crystallinity on wear behavior of PTFE composites. *Wear*, 307(1–2), pp.81–86. Available at: <http://linkinghub.elsevier.com/retrieve/pii/S0043164813004729>.
- Eiss, N.S. & Potter, J.R., 1985. Fatigue Wear of Polymers. In *Polymer Wear and Its Control*. ACS Symposium Series. American Chemical Society, pp. 4–59. Available at: <http://dx.doi.org/10.1021/bk-1985-0287.ch004>.
- Findik, F., 2014. Latest progress on tribological properties of industrial materials. *Materials and Design*, 57, pp.218–244. Available at: <http://dx.doi.org/10.1016/j.matdes.2013.12.028>.
- Halley, P.J. & Mackay, M.E., 1994. The effect of metals on the processing a slit die of LLDPE through. , 38(February), pp.41–51.
- Jintang, G., 2000. Tribochemical effects in formation of polymer transfer film. *Wear*, 245(1–2), pp.100–106.
- Konovalova, I.O., Ing, P. & Suchanek, J., 2012. Significance of Polymer Nanocomposites in Triboengineering Systems. *Proceedings of the 4th International Conference NANOCON 2012*.
- Lancaster, J.K., 1969. 223 Abrasive Wear of Polymers*. *Materials Science*, 4, pp.223–239.
- Lancaster, J.K., 1972. Polymer-based bearing materials - The role of fillers and fibre reinforcement. *Tribology*, 5(6), pp.249–255.
- Lee, K.J. et al., 2007. The influence of carbon fiber orientation on the mechanical and tribological behavior of carbon fiber/LCP composites. *Materials Chemistry and Physics*, 102(2–3), pp.187–194.

- Liu, X.-X. et al., 2007. An investigation on the friction of oriented polytetrafluoroethylene (PTFE). *Wear*, 262(11–12), pp.1414–1418. Available at: <http://linkinghub.elsevier.com/retrieve/pii/S0043164807002025>.
- Liu, X.-X. et al., 2005. Study on Tribological Properties of Polytetrafluoroethylene Drawn Uniaxially at Different Temperature. *Macromolecular Materials and Engineering*, 290(3), pp.172–178. Available at: <http://doi.wiley.com/10.1002/mame.200400213>.
- Materials, A., 2012. Carbon Steel C1018 Specifications. *N/A*, p.N/A.
- McMasterCarr, 2016a. Inconel 625 Specifications. *N/A*, p.N/A.
- McMasterCarr, 2016b. Naval Brass 485. *N/A*, p.N/A.
- McMasterCarr, 2016c. Stainless Steel 316SS Specification. *N/A*, p.N/A.
- Myshkin, N.K., Petrokovets, M.I. & Kovalev, A. V., 2005. Tribology of polymers: Adhesion, friction, wear, and mass-transfer. *Tribology International*, 38(11–12 SPEC. ISS.), pp.910–921.
- Novak, R. & Polcar, T., 2014. Tribological analysis of thin films by pin-on-disc: Evaluation of friction and wear measurement uncertainty. *Tribology International*, 74, pp.154–163.
- Onodera, T. et al., 2014. Effect of tribochemical reaction on transfer-film formation by poly(tetrafluoroethylene). *Journal of Physical Chemistry C*, 118(22), pp.11820–11826.
- Person, T.J., 1997. The effect of die materials and pressure-dependent slip on the extrusion of linear low-density polyethylene. *Journal of Rheology*, 41(2), p.249. Available at: <http://link.aip.org/link/?JOR/41/249/1&Agg=doi>.
- Petrica, M. et al., 2015. Tribological investigations on virgin and accelerated aged PE-UHMW. *Tribology International*, 87, pp.151–159. Available at: <http://linkinghub.elsevier.com/retrieve/pii/S0301679X15000699>.
- Sawyer, W.G. et al., 2003. A study on the friction and wear behavior of PTFE filled with alumina nanoparticles. *Wear*, 254(5–6), pp.573–580.
- da Silva, R.C.L., da Silva, C.H. & Medeiros, J.T.N., 2007. Is there delamination wear in polyurethane? *Wear*, 263(7–12 SPEC. ISS.), pp.974–983.
- Tanaka, K., Uchiyama, Y. & Toyooka, S., 1973. The mechanism of wear of polytetrafluoroethylene. *Wear*, 23(2), pp.153–172.
- Tzanakis, I. et al., 2013. Experimental and analytical thermal study of PTFE composite sliding against high carbon steel as a function of the surface roughness, sliding velocity and applied load. *Wear*, 303(1–2), pp.154–168.
- Unal, H., Sen, U. & Mimaroglu, a., 2004. Dry sliding wear characteristics of some industrial polymers against steel counterface. *Tribology International*, 37, pp.727–732.
- Wenzhong, N., 2015a. The effect of carbon fibers and carbon nanotubes on the mechanical properties of polyimide composites. *Journal of Thermoplastic Composite Material*, 28(11), pp.1572–1582.

- Wenzhong, N., 2015b. The effect of carbon fibers and carbon nanotubes on the mechanical properties of polyimide composites. *Journal of Thermoplastic Composite Material*, 28(11), pp.1572–1582. Available at: <http://www.springerlink.com/index/075K4NX1320U804J.pdf>.
- Williams, J., 2005. *Engineering tribology*, Cambridge University Press.
- Yamamoto, Y. & Hashimoto, M., 2004. Friction and wear of water lubricated PEEK and PPS sliding contacts Part 2. Composites with carbon or glass fibre. *Wear*, 257(1–2), pp.181–189.
- Zhang, G. et al., 2015a. Impact of counterface topography on the formation mechanisms of nanostructured tribofilm of PEEK hybrid nanocomposites. *Tribology International*, 83, pp.156–165. Available at: <http://linkinghub.elsevier.com/retrieve/pii/S0301679X14004174>.
- Zhang, G. et al., 2015b. Impact of counterface topography on the formation mechanisms of nanostructured tribofilm of PEEK hybrid nanocomposites. *Tribology International*, 83, pp.156–165.
- Zhang, J., 2011. The effect of carbon fibers and carbon nanotubes on the mechanical properties of polyimide composites. *Mechanics of Composite Materials*, 47(4), pp.1–4. Available at: <http://www.springerlink.com/index/075K4NX1320U804J.pdf>.
- Zhao, G. et al., 2012. Friction and wear of fiber reinforced polyimide composites. *Wear*, 301, pp.122–129.
- Zhou, S. et al., 2013. Effect of carbon fiber reinforcement on the mechanical and tribological properties of polyamide6/polyphenylene sulfide composites. *Materials & Design*, 44, pp.493–499. Available at: <http://www.sciencedirect.com/science/article/pii/S0261306912005687>.

Appendix

The following tribometer and LabView program was fabricated specifically for the experiments conducted in this study.



Figure A1 - Tribometer fabricated specifically for this study.



Figure A2 - Close up view of a mounted sample



Figure A3 - Unworn polymer sample and C1018 Washer



Figure A4 - Worn polymer sample and C1018 washer.

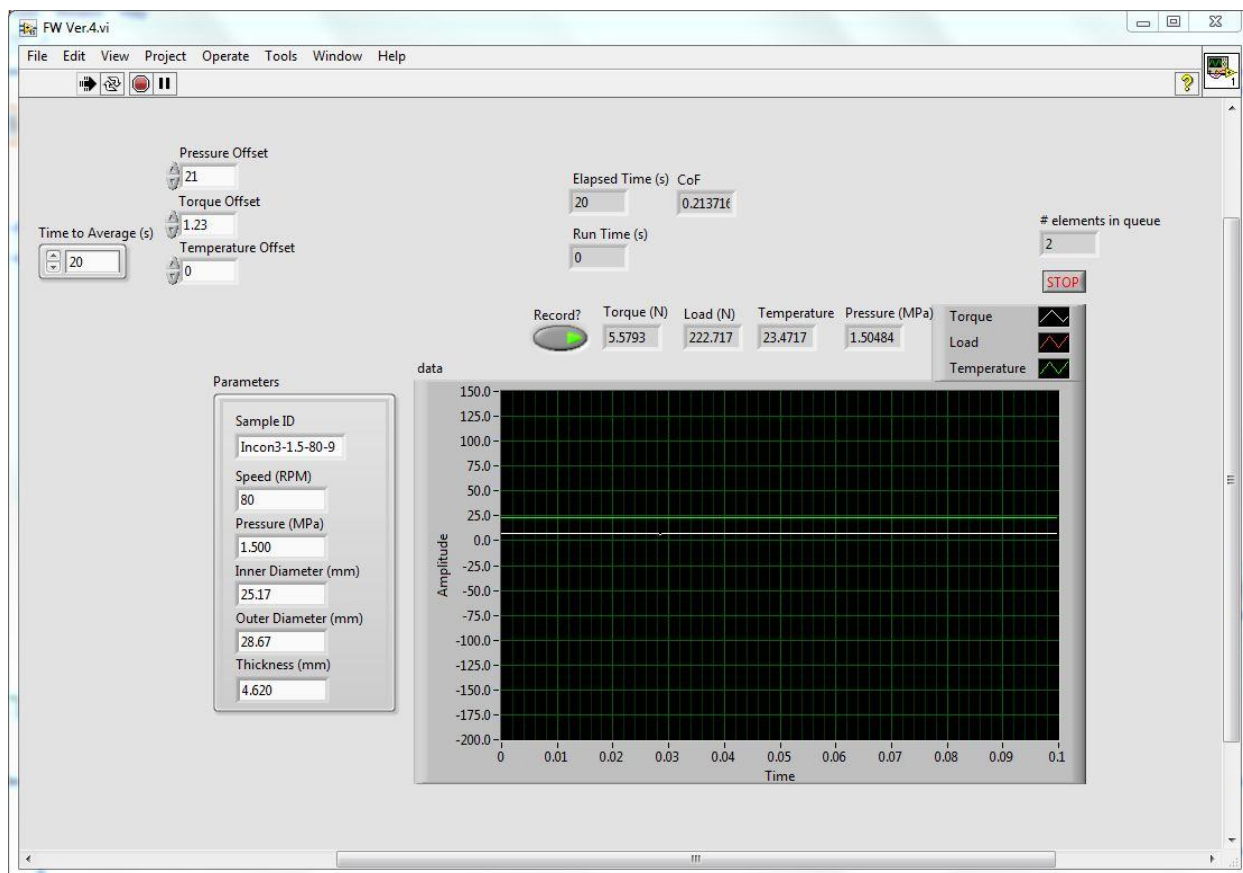


Figure A5 - LabView program main screen.

The following table contains the average mass lost for each polymer-metal system in its stable and unstable state.

Table A1 - Comparison of average CoF and absolute wear of polymer-metal system

	Average CoF	Sample Wear (mg)	Washer Wear (mg)	Total Wear (mg)
C1018 Stable	0.252±0.015	0.8±0.5	0.3±0.2	1.1±0.4
C1018 Unstable	0.234±0.039	1.0±0.3	0.2±0.2	1.1±0.4
Brass Stable	0.236±0.015	0.6±0.3	0.5±0.2	1.0±0.5
Brass Unstable	0.237±0.016	0.4±0.1	0.5±0.3	0.9±0.3
Inconel Stable	0.197±0.012	1.2±0.7	0.3±0.2	1.5±0.7
Inconel Unstable	0.188±0.025	0.9±0.3	0.5±0.2	1.5±0.4
316SS Stable	0.215±0.029	1.1±0.6	0.3±0.2	1.3±0.7
316SS Unstable	0.206±0.019	0.9±0.3	0.3±0.2	1.2±0.4